MARCH 1957 VOLUME 1 (1957) No. 2

GREGG M. SINCLAIR LIBRARY
UNIVERSITY OF HAWAII
8-7-63

NUCLEAR INSTRUMENTS

A JOURNAL ON ACCELERATORS, INSTRUMENTATION AND TECHNIQUES IN NUCLEAR PHYSICS

EDITOR K. SIEGBAHN – UPPSALA

CONTENTS

G. GHIGO and I. F. QUERCIA, Field stabilization in a D.C.-A.C. magnet of a synchrotron . . . 57
M. A. MEYER, Pulse-lengthener circuits . . . 62
C. A. J. KRITZINGER, An apparatus for measuring the speed of pneumatically transported grains by means of radioactivity . . . 66
W. P. BALL, R. BOOTH and M. MACGREGOR, Temperature coefficients of scintillating systems 71
R. V. GÅSSTRÖM, A very fast pulse-height analyser with independent uptake, sorting and storage of information . . . 75
N. E. BOOTH and G. W. HUTCHINSON, Fine time-structure of beams from the Birmingham proton synchroton . . . 80
P. B. TREACY and N. F. BOWKETT, A target box for bombardment of CF_4 in gaseous or solid form 86
S. J. GOLDSACK, Two target operation of a proton-synchroton . . . 90
F. G. P. SEIDL, H. PALEVSKY, D. J. HUGHES and R. L. ZIMMERMAN, Modification of the Brookhaven fast chopper . . . 92
I. CORNIDES, J. ROÓSZ and A. SIEGLER, Two lithium ion sources for accelerators . . . 94
PER-ARNE TOVE, Electronic time analyzer applied to the measurement of the half-lives of metastable nuclear states . . . 95
R. R. WILSON, Precision quantameter for high energy X-rays . . . 101
T. R. GERHOLM, T. LINDQVIST and H. DE WAARD, Multi coincidence goniometer for angular correlation measurements . . . 107
Book Review . . . 112

NORTH-HOLLAND PUBLISHING COMPANY AMSTERDAM

NUCLEAR INSTRUMENTS

A journal on accelerators, instrumentation and techniques in nuclear physics

EDITOR: K. SIEGBAHN, UPPSALA

EDITORIAL BOARD:

J. B. ADAMS (CERN)
E. AMALDI (Rome)
H. L. ANDERSON (Chicago)
K. T. BAINBRIDGE (Cambridge, Mass.)
C. J. BAKKER (CERN)
P. R. BELL (Oak Ridge)
R. E. BELL (Montreal)
A. BERTHELOT (Saclay)
H. BRINKMAN (Groningen)
S. DE BENEDETTI (Pittsburgh)
M. DE HEMPTINNE (Louvain)
A. DE-SHALIT (Rehovoth)
S. DU TOIT (Pretoria)
M. DEUTSCH (Cambridge, Mass.)
W. GENTNER (CERN)
P. C. GUGELOT (Amsterdam)
H. HALBAN (Paris)
O. HAXEL (Heidelberg)
P. HUBER (Basel)
D. J. HUGHES (Brookhaven)
S. KIKUCHI (Tokyo)
J. KOCH (Copenhagen)
S. LIVINGSTON (Cambridge, Mass.)
E. M. MCMILLAN (Berkeley)
P. B. MOON (Birmingham)
M. L. OLIPHANT (Canberra)
W. PAUL (Bonn)
A. S. RAO (Bombay)
G. SALVINI (Rome)
P. SAVIĆ (Belgrade)
P. SCHERRER (Zürich)
CH. SCHMELZER (CERN)
H. W. B. SKINNER (Liverpool)
R. TANGEN (Blindern)
O. WERNHOLM (Stockholm)
D. TAYLOR (Harwell)
G. VON DARDEL (CERN)
R. R. WILSON (Cornell)
S. D. WINTER (Saclay)

Contributions may be sent to the Editor, Professor K. Siegbahn, Institute of Physics, the University of Uppsala, either directly or through the intermediary of one of the members of the Editorial Board of the country or region in which the author is working. Contributions may be written in English, French or German, with an abstract in English.

Books for review should be sent to Professor Siegbahn.

Nuclear Instruments is published in bi-monthly issues. The subscription price of a volume of 360 pages is $ 17.00 (130 s), postage free.

Subscriptions should be sent to the publishers, North-Holland Publishing Company, P.O.Box 103, Amsterdam or to any subscription-agent. Subscriptions for U.S.A. are to be sent exclusively to Interscience Publishers, Inc., 250 Fifth Avenue, New York, 1 N.Y.

NUCLEAR INSTRUMENTS 1 (1957) 57–61; NORTH-HOLLAND PUBLISHING CO. – AMSTERDAM

FIELD STABILIZATION IN A D.C.—A.C. EXCITED MAGNET OF A SYNCHROTRON

G. GHIGO and I. F. QUERCIA

Istituto Nazionale di Fisica Nucleare Sezione Acceleratore, Roma

Received 28 October 1956

The shape of the magnetic field of an Electron-Synchrotron is quite critical at injection. If the machine is fed with an A.C. current and with a bias D.C. current, the shape of the field at injection is quite sensitive to the values of the peak A.C. current and of the D.C. current. A device is described that is sensitive to the difference between peak A.C. and D.C. current and which keeps this difference constant by controlling the value of the D.C. current. The apparatus was applied to model magnets of the 1 GeV Italian Electron-Synchrotron, and is planned for controlling the supply of the Synchrotron.

1. In the design of an Electron-Synchrotron much care must be given to the values of the magnetic parameters at the time of injection. In fact the field in the gap at injection is only a few gauss, and both the remanent field and the eddy currents have a very large effect on the space and time distribution of the field. For keeping the field distribution the same in every cycle it is very important to keep constant the value of the peak reverse field, and the value of the rate of rise of the field at injection time.

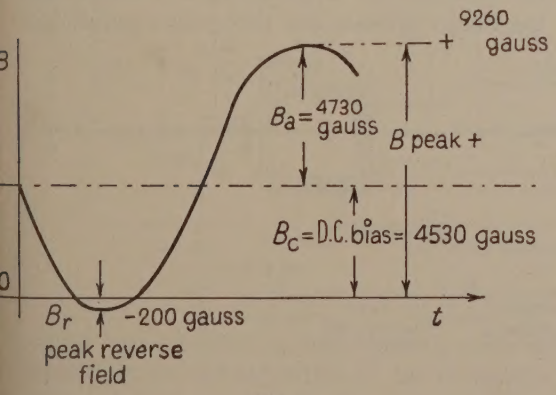

Fig. 1

In the project for 1 GeV italian Electron-Synchrotron (4) we shall excite the magnet with a 20 c/s sinusoidal current and with a bias direct current. The resulting magnetic field in the gap will be of course composed of an A.C. sinusoidal component and a D.C. component. As fig. 1 shows, the peak reverse value of the field B_r, is just the difference between the peak value of the A.C. component B_a, and the value of the D.C. component B_c. Suppose that we want a peak positive value of the field of 9260 gauss, and a peak reverse field $B_r = 200$ gauss: this gives $B_a = 4730$ gauss and $B_c = 4530$ gauss.

If we will be able to stabilize the D.C. current and the A.C. current feeding the magnet in such a way that independent variations of B_a and B_c will be limited at $\pm 0.1\,\%$, the possible variation of B_r will still be about $5\,\%$. Moreover this variation of B_r is accompanied by a change of about $2.5\,\%$ of the rate of the rise

$$\dot{B} = \frac{dB}{dt}$$

of the field at injection.

To reach a $0.1\,\%$ stability in the performance of the heavy machinery that supplies the magnet is not very easy, and to ask for a higher degree of stability is very expensive, or may be impossible.

For this reason we considered the possibility of approaching the problem in a quite different way. We started from the observation that what we need is some kind of stabilization of the reverse peak value of the magnetic field; we can let the A.C. magnetic field vary in a reasonable

range if we are able to track the A.C. field with the D.C. field in such a way that the peak reverse value of the total field is mantained within allowed limits.

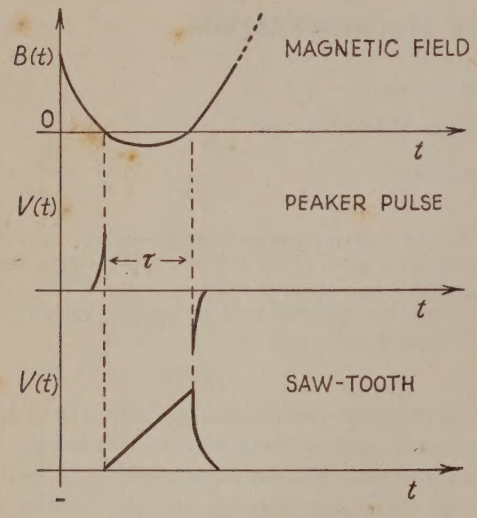

Fig. 2

This of course leads to the problem of measuring the value of the peak reverse field.

The most obvious way to measure it, seems to be to measure the difference between the peak value of the A.C. current, and the value of the D.C. current. Unfortunately the currents to be measured are so high that a voltage drop of 1 Volt corresponds to some kilowatt of power, and we can not hope to be able to measure D.C. voltages of less than 1 Volt with an accurancy better than 10 mV. In fact any electronic device for measuring D.C. voltages is affected by a drift of some millivolts which can not be easily suppressed. For these reasons we found it more convenient to leave the idea of measuring the components of the current feeding the magnet and to use a device sensitive directly to the peak value of the reverse magnetic field.

2. The device consists of a probe containing a peaking strip surrounded by a pick-up coil. The probe is placed in the fringing field of the synchrotron magnet. As is well known (see for instance ref. [1]) a voltage pulse is generated by the peaking strip in the pick-up coil, every time the magnetic field crosses the null value. Pulses change their polarity according to the sign of the time derivative of the magnetic field.

Following the wave forms shown in fig. 2, the first positive pulse starts a saw-tooth wave form generator, while the second negative pulse stops the saw-tooth. The peak value of the saw-tooth wave results to be function of the peak reverse value of the magnetic field.

Through a vacuum tube peak voltmeter, the peak value of the saw-tooth is compared with a reference voltage; the error voltage drives a power amplifier that controls the excitation current of the D.C. generator feeding the magnet. The block diagram of the apparatus is shown in fig. 3. The control loop acts as follows: suppose the peak reverse magnetic field is increasing; the time τ between the two peaker pulses also increases; the peak of the saw-tooth wave is raised and the voltage V_f developed by the peak voltmeter is no more equal to the reference

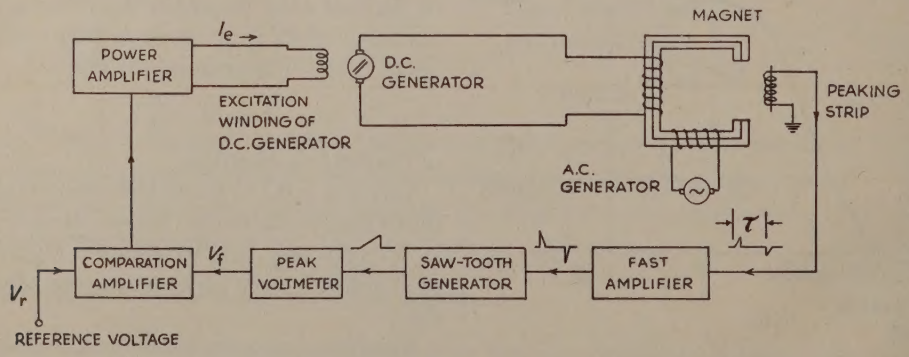

Fig. 3

[1]) G. Diambrini, Nuovo Cimento X 3 (1956) 336.

voltage V_r. The error voltage $(V_f - V_r)$ drives the current amplifier resulting in an increase dI_e of the excitation current of the D.C. generator. The D.C. bias of the magnet is raised, and the peak value of the reverse field is adjusted to the correct value.

3. It is easy to show that the effect of the device is to reduce the variation dB_r of the peak reverse field as consequence of a variation dB_a of the peak value of A.C. field, according to the formula:

$$dB_r = \frac{dB_a}{1+L}$$

where L is the gain of the feed-back loop. (see for instance ref. [2]). Of course, according to the general rules of feed-back loops[3]), the value of the loop gain L is limited by the Nyquist stability criterion. In our case part of the loop frequency response of the open loop to be of the "dominant lag" type (see e.g. (2)).

It can be demonstrated that a loop like this is stable if the zero frequency loop gain $L(0)$, is limited by the following relation:

$$L(0) < \frac{T}{\theta} .$$

The latter equation shows that we must choose a compromise between the stabilization factor $1 + L$ and the response speed of the loop.

If we want to increase the stabilization effect of the system, we must increase the time-lag T; as a consequence we loose any control over fast transsient in the value of the peak reverse field B_r.

4. We have applied the stabilization system described in the previous paragraphs to a model

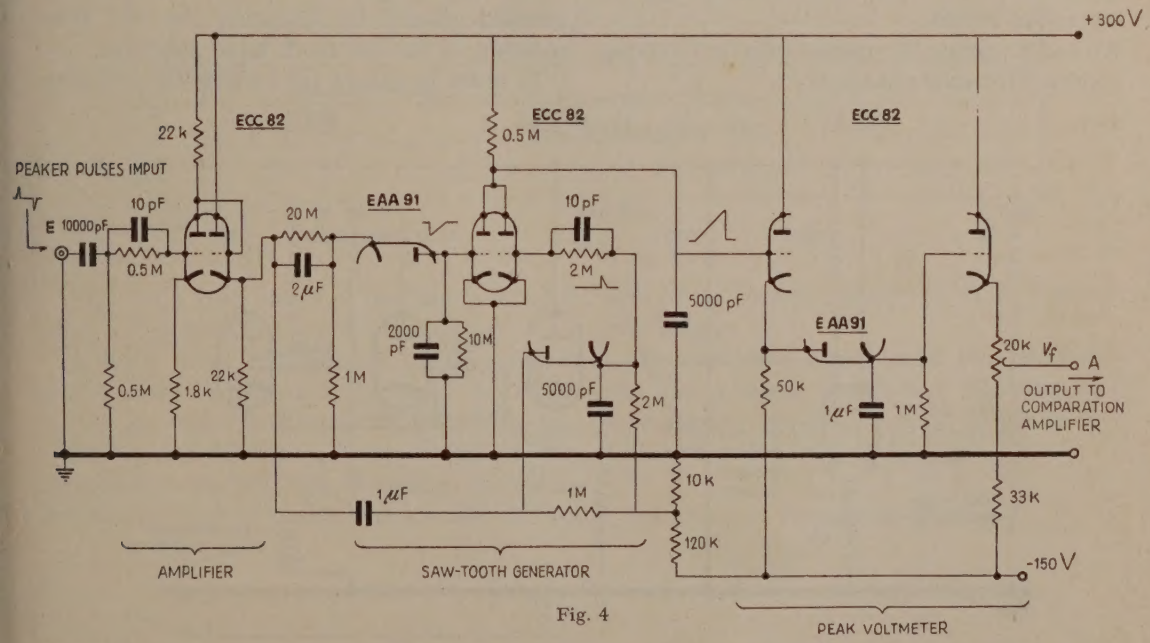

Fig. 4

carries an intermittent information, with a repetition rate corresponding to the frequency of the A.C. generator supplying the magnet. This fact introduces an unavoidable delay time θ between two successive informations.

Moreover we can suppose that the electromechanical part of the system introduces a very big time lag T, so that we can consider the magnet of the 1 GeV electronsynchrotron to be built in Frascati[4]). The magnet excitation coil

[2]) J. G. Thomason, Linear Feed-back Analysis (Mc Graw Hill, 1955).

[3]) H. W. Bode, Network Analysis and Feed-back amplifiers design, (D. van Nostrand Co., 1953).

[4]) G. Salvini, Caratteristiche dello Elettrosincrotrone da 1000 MeV (I.N.F.N. Sezione Acceleratore G. 19, 31 Ottobre 1955).

was paralleled by a condenser bank in resonance at 50 c/s.

The Q value of the resonating LC circuit was about 20. The A.C. excitation current was taken from a transformer directly from the mains.

The D.C. bias excitation current was supplied from a 13 kW generator driven by an asynchronous motor. The field of the D.C. generator, was supplied by a smaller 0.2 kW, D.C. generator. The field of this small D.C. generator was supplied from the electronic power amplifier to be described later.

Variations of the peak value of the A.C. field of the order of $\pm$ 10% were observed, due the instability of both the voltage and frequency of the mains. In fact the A.C. current in the magnet was very sensitive to the value of the frequency as a consequence of the high Q value of the LC resonating circuit.

We had to operate the magnet with the following approximate values of the field:

Peak positive value of the field $\approx$ 8500 gauss.

Peak reverse value of the field $\approx$ 200 guass.

It follows that the A.C. component of the field has a peak value $B_a \approx 4{,}350$ gauss, and the D.C. component has a valued of $B_c \approx 4150$ gauss.

A change of only -5% of the B_a value causes the reverse field to disappear completly, with the consequence of changing drastically the remanent field in the iron of the magnet, and of course the slope of the field at injection.

As sensitive element we used a Mu-metal wire of 0.05 mm diameter and about 40 mm length. This peaking strip was surrounded in the middle by a 400 turns pick-up coil. Pulses of about 60 mV induced in the pick-up coil, were amplified by a conventional fast amplifier of gain 100, and injected in the electronic device of fig. 4. The peak value V_f of the saw-tooth wave form was compared with a reference voltage V_r in the electronic device of fig. 5, and the resulting error voltage drove the power amplifier (two 807 valves).

The zero frequence loop gain $L(0)$ can be changed simply by changing the RC time constant of the saw-tooth wave generator.

In order to choose the correct value of loop

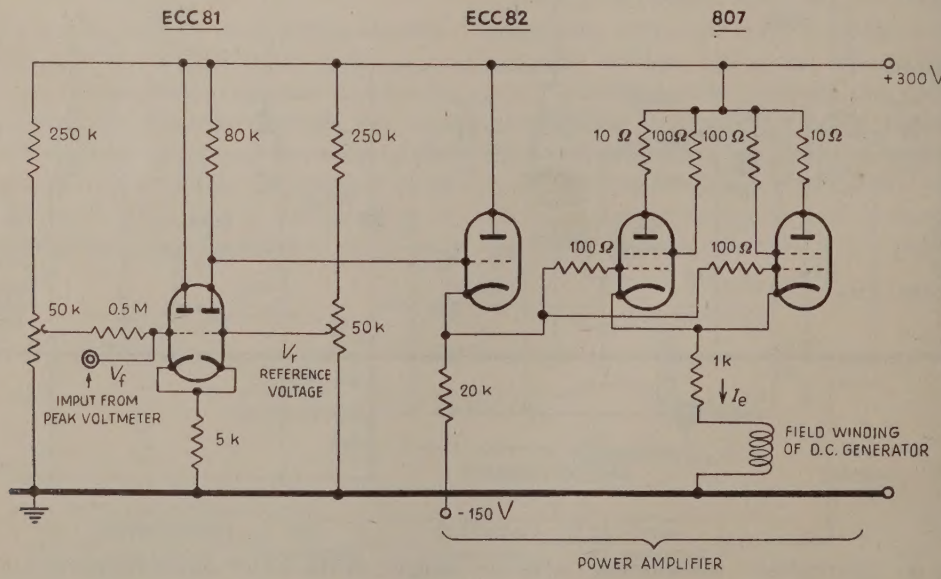

Fig. 5

gain, supposing that the main lag-time T is introduced by the chain: D.C. exciter—D.C. Generator—Magnet, we measured the rate of rise of the magnetic field in the gap due to a step pulse of current supplied by the power amplifier.

We observed a rise time corresponding to

$T = 0.9$ seconds. Because the delay between two successive informations corresponds to 1/50 of a second, according to the discussion of § 3, we decided to have a loop gain $L(0) = 30$.

In the operating conditions we had a loop gain of:

$$L(0) = 32.5.$$

With this device the long term stability of the peak reverse value of B_r was observed to be about $\pm$ 10%.

to control the field in the magnet of our Electron-Synchrotron.

Of course it is possible to use other quantities, than the time τ, for measuring and controlling the shape of the field at injection. For istance the Cornell Synchrotron Group developed a device[5]) that samples the value of

$$\dot{B} = \frac{dB}{dt}$$

at injection time, and controls the A.C. compo-

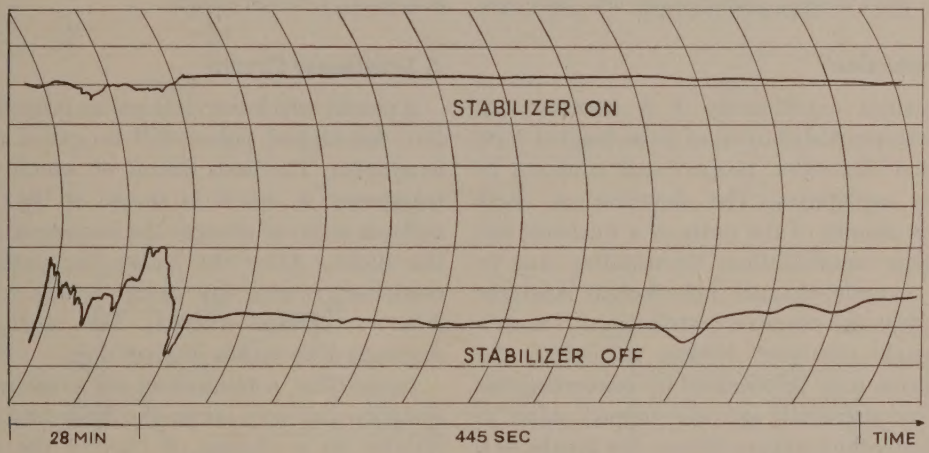

Fig. 6

Fig. 6 is a time record of the time interval τ with and without the stabilization device.

5. With some modification in the output power stage we have used the device described in the previous paragraphs for stabilizing the peak reverse field in a bigger model of our Synchrotron magnet. We obtained good results, and now we hope to be able with a similar device

nent of the current feeding the 1 GeV Synchrotron magnet.

We would like to emphasize that our device can find a wider application whenever it is necessary to control the relative values of a D.C. and an A.C. current.

[5]) A. Silverman, Private Communication.

NUCLEAR INSTRUMENTS 1 (1957) 62–65; NORTH-HOLLAND PUBLISHING CO. – AMSTERDAM

PULSE-LENGTHENER CIRCUITS

M. A. MEYER

Physics Department, University of Potchefstroom, South Africa

Received 28 August 1956

Existing and new circuits are discussed which converts pulses of short duration proportionally into flat-topped pulses of which the duration varies from a few tenths of a microsecond to several seconds.

1. Introduction

In certain experiments it is necessary to determine the distribution of pulse heights from ionization chambers, proportional counters or electron multipliers. The duration of these pulses is usually of the order of a microsecond. After some amplification, these pulses may be fed to a multi-channel pulse-height analyzer which gives the required distribution. If such a pulse-height analyzer is not available, the distribution may be obtained by converting the pulses proportionally into flat-topped pulses of a duration which ranges from a few tenths of a microsecond to several seconds. One method of obtaining the distribution is to feed these flat-topped pulses to the Y-axis of an oscilloscope. An intensifying gate is applied to the Z-axis during the flat portion of the pulse with the result that only the top part of the pulse is visible on the screen. With a slow sweep, the spectrum of the pulses is represented by dots on the screen. The departure of each from the base line being proportional to the amplitude of the incident pulse. These dots are recorded on a photographic film from which the distribution can be determined. When this method is used, the duration of the flat topped pulses usually varies between a few microseconds to a few hundred microseconds. A second method to register the size of the pulses is to use a mechanical recorder such as the Esterline-Angus recorder or a vacuum-tube voltmeter. In this case, the duration of the flat-topped pulses must be of the order of a few seconds.

2. Lengthener Circuits

A circuit which converts pulses proportionally into flat-topped pulses will be called a pulse-lenghtener. The basic circuit on which a pulse-lengthener is based is shown in fig. 1. The cathode follower charges the condenser through the diode. After the pulse has passed, the condenser retains the charge it has collected. After a certain interval, the condenser is discharged by means of a restorer.

In practice, a fraction of the pulse is lost in the potential drop across the diode and another fraction in a change of bias of the cathode follower. Pulse-lengtheners are included in circuits at high signal levels to avoid objectionable non-linearities in diodes.

The average current which must be supplied by the cathode follower in order to charge a condenser to a potential of ΔV in the time Δt is given by $C\Delta V/\Delta t$. If a tube is employed which can supply a maximum current of 50 mA before drawing grid current and if the pulse rises in 0.1 microseconds, a condenser of 100 pF can be charged to 50 volts. The capacity of the storage condenser is therefore limited by the maximum current which the cathode follower is able to furnish without drawing grid current. If it is required to charge a larger condenser, ΔV must either be smaller or Δt larger. In practice ΔV can be made smaller by connecting the diode to a tap on the cathode resistance. In this manner condensers of which the capacity is as large as 1000 pF can be charged in the required time.

It was mentioned previously that, when a

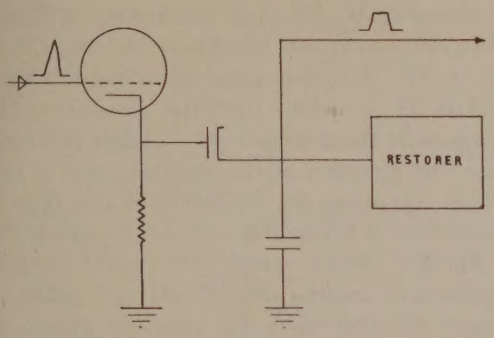

Fig. 1

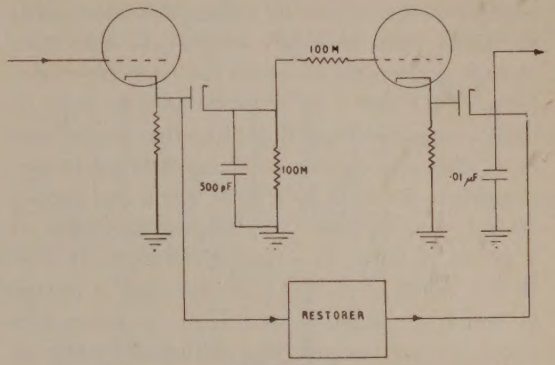

Fig. 2

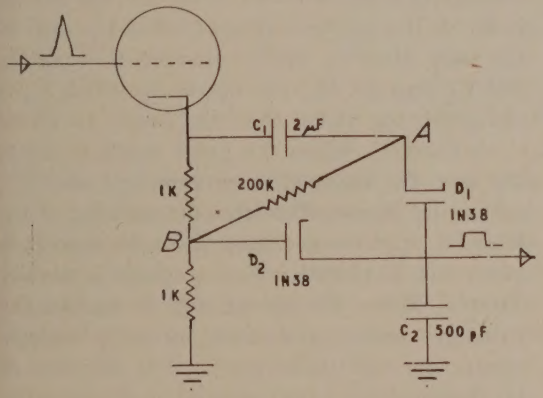

Fig. 3a

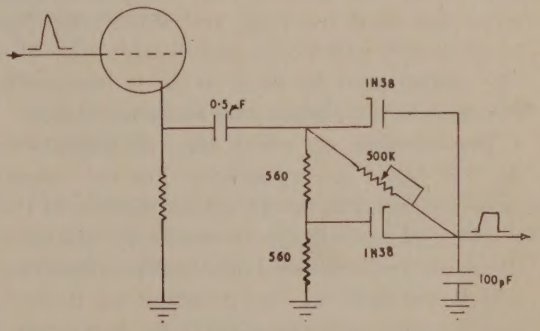

Fig. 3b

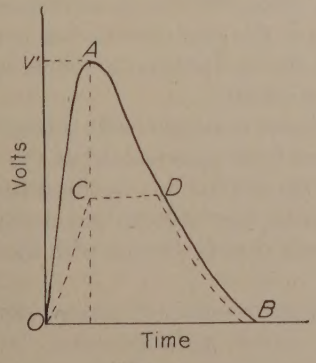

Fig. 4

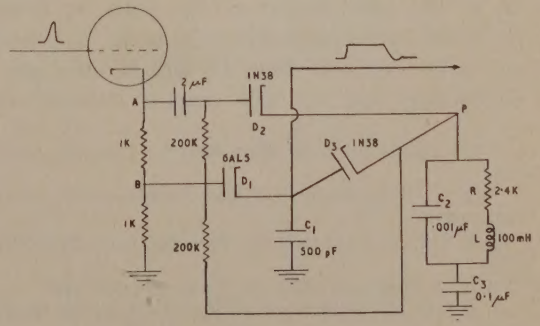

Fig. 5

vacuumtube voltmeter or a pen-recorder is used to register the size of the pulses, the duration of the pulse must be a few seconds. In this case, storage condensers of which the capacity varies between 0.1 and 1 μF must be used in order to reduce leakage effects. It is clear that a condenser of this size cannot be charged in 0.1 microseconds to 50 volts by a tube which can supply 50 mA. Such a tube can charge a condenser of 1 μF to 50 volts. in a time given by $C\ \Delta V/i = 10^{-6} \times 50/50 \times 10^{-6} = 1$ millisecond. A circuit in which a condenser of 0.1 μF is charged in about one milliseconds was published by Dewan and Allen[1]) (fig. 2). The restorer was triggered by the incoming pulse. A similar circuit was described by Elmore and Sands[2]).

Lengthener circuits which convert incoming pulses into flat-topped pulses of which the duration is the same as that of the incoming pulse was used by West and Mann[3]) (fig. 3a). Hunt *et al.*[4]) and Foote and Koch[5]) (fig. 3b). The circuit used by Hunt *et al.* is practically the same as the one used by Foote and Koch.

The principle on which the two circuits in fig. 3 is based is very similar. For this reason only the circuit in fig. 3a will be discussed. The anodes and the cathodes of the diodes will be at the same potential and the storage condenser will be charged to the potential at B. If a positive pulse of the form OAB (fig. 4) is applied to the grid of the tube, a pulse will appear at both A and B. The pulse at A will have the form OAB and will be larger than the pulse at B. The condenser C_2 will be charged through the diode D_2 to the same height as the pulse at B as indicated by the dotted line OC in fig. 4. When the pulse starts to drop, D_2 will become non-conducting and C_2 will remain charged as indicated by the dotted line CD. As soon as the potential at A reaches the potential to which C_2 is charged, D_1 becomes conducting and discharges C_2 as shown by the dotted line DB in fig. 4. The flattened pulse then has the form OCDB. It is evident from the above that the duration of the flattened pulse cannot be longer than the duration of the original pulse, a fact which represents the limitation of this type of lengthener. A favourable aspect is its simplicity.

Another circuit which was found to give satisfactory results when flat-topped pulses of longer duration than the incoming pulses are required, is shown in fig. 5. The duration of the pulses can be varied between a few microseconds to several tens of microseconds. This circuit is essentially a modification of the circuits shown in fig. 3. If a positive pulse is fed to the grid of the tube, then C_1 will be charged through D_1 and C_2 through D_2; the height to which C_2 is charged being higher than the height to which C_1 is charged. When the pulse starts to drop, D_1 and D_2 become non-conducting and C_1 retains its charge. The circuit consisting of C_2, R and L starts to oscillate. The resistance R is given such a value that the oscillation is heavily damped. When the potential at P reaches the value to which C_1 is charged, then D_3 becomes conducting and discharges C_1. The duration of the flattened pulse can be varied by changing the values of C_2 or L. Increasing C_2 and/or L, increases the duration of the flattened pulse. Increasing C_1 also increases the duration of the flattened pulse, but this is accompanied by an attenuation. The condenser C_3 does not affect the period of the oscillations; it simply isolates the oscillating circuit.

A condenser in parallel with a large resistance could have been used instead of the oscillating circuit. This method has the disadvantage that the decreasing part of the flattened pulse becomes much longer than is the case with the oscillating circuit.

If flattened pulses of longer duration are required, other methods must be used to discharge the condenser. The method used by Dewan and Allen[1]) and by Bernstein *et al.*[6]) is

[1]) J. T. Dewan and K. W. Allen, Rev. Sci. Instr. **21** (1950) 823.

[2]) W. C. Elmore and M. Sands, Electronics (McGraw-Hill, 1949).

[3]) H. I. West and L. G. Mann, Rev. Sci. Instr. **25** (1954) 129.

[4]) W. A. Hunt *et al.*, Rev. Sci. Instr. **25** (1954) 268.

[5]) R. S. Foote and H. W. Koch, Rev. Sci. Instr. **25** (1954) 746.

[6]) W. Bernstein, R. L. Chase and A. W. Schardt, Rev. Sci. Instr. **24** (1953) 437.

to discharge the condenser by means of a tube. A modification of the circuits used by these authors is shown in fig. 6. The duration of the

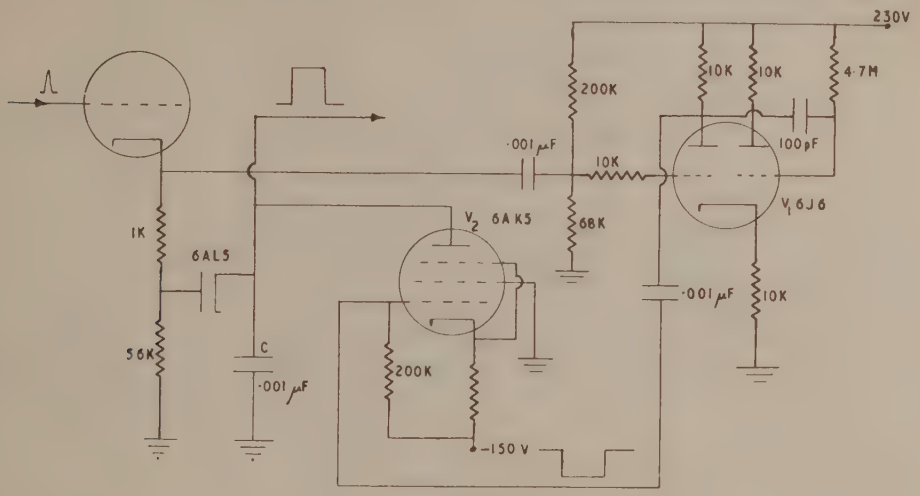

Fig. 6

flattened pulses from this circuit is about sixty microseconds. The duration can be varied from about a microsecond to several hundred microseconds by a suitable choice of the circuit constants of the univibrator circuit. Positive pulses from the cathode follower triggers the univibrator which delivers a negative pulse to the grid of the tube V_2 which is normally conducting. V_2 again conducts and discharges C at the end of the negative pulse from the univibrator.

This is part of a program which is assisted by the South African Council for Scientific and Industrial Research.

NUCLEAR INSTRUMENTS 1 (1957) 66–70; NORTH-HOLLAND PUBLISHING CO. – AMSTERDAM

AN APPARATUS FOR MEASURING THE SPEED OF PNEUMATICALLY TRANSPORTED GRAINS BY MEANS OF RADIOACTIVITY

C. A. J. KRITZINGER

Division of Nuclear Physics, National Physical Laboratory, Pretoria

Received 1 October 1956

In studies of the pneumatic transport of granular material it is necessary to measure the speed of individual grains. In a specific investigation a 2.5 cm diameter tube was used and an accuracy of at least 3% over a distance of 1.8 meters for speeds up to 18 m/sec was required.

As photographic methods yielded rather disappointing results, the problem was solved by activating individual grains with Caesium 137 and using shielded scintillation counters 1.8 meters apart as triggers to start and stop an electronic clock, from which the speed could then be easily calculated.

From the accuracy requirements it is at once evident that scintillation counters should be used because of their higher efficiency as compared to Geiger-Müller tubes. It follows that in order to obtain 0.3% accuracy over 1.8 meters it would mean that the effective collimator width used should not be more than about 2 cm and that a reasonable number of pulses should be available in the time a grain passes the collimator. A minimum of 12 pulses gives a required count rate of at least 4 000 counts/sec. when the grain is stationary before the collimator. Rough calculations and some experiments on the required collimator length showed that the activity on an individual grain should be about 0.5 millicurie. Fig. 1 shows the mechanical construction of the collimator, and in fig. 2 the curves giving the count rate as a function of the position of a 0.5 millicurie source is shown. Curve A was obtained with the source passing along the *inside* of the tube nearest the scintillation crystal, whereas B was made with the source along the *inside* of the tube remotest from the detector.

The set of curves of fig. 3 follows from fig. 2 where A′ and B′ are simply the integral curves of A and B calculated for the maximum speed. The curves $\bar{A}'$, $\underline{A}'$, B′ and $\underline{B}'$ allow for statistical variations and are $A \pm \sqrt{A}$ and $B \pm \sqrt{B}$ respectively.

If the trigger circuit is now set to trigger only when the count rate exceeds that given by the time of minimum count rate, i.e., 3600/sec then ε is the maximum positional error, which for the conditions shown, is 1.64%. The timing error may be 0.5 millisec, i.e. 0.5%, as a 2 kc oscillator is used and individual cycles are counted. The absolute accuracy of the frequency is better than 0.5% and hence the overall accuracy of the whole system is better than the required 3%.

As the grains to be detected are moving in a brass tube, a γ-emitter is required. Radio-iodine was used originally and proved to be quite successful on the more substantial grains. With tapioca, however, (which was eventually extensively used) considerable swelling occurred which rendered the activated tapioca aerodynamically dissimilar to the unactivated. High specific activity Caesium 137 in 6N HNO_3 was used instead. The particle was soaked in the active solution and dried giving an activity of about 0.5 mc. To prevent the formation of active dust the particles were dipped in a solution of perspex and dried. No activity was detected in the dust from the tapioca after the experiments and the activated particles were found to be well within the statistical spread of untreated particles in size and shape.

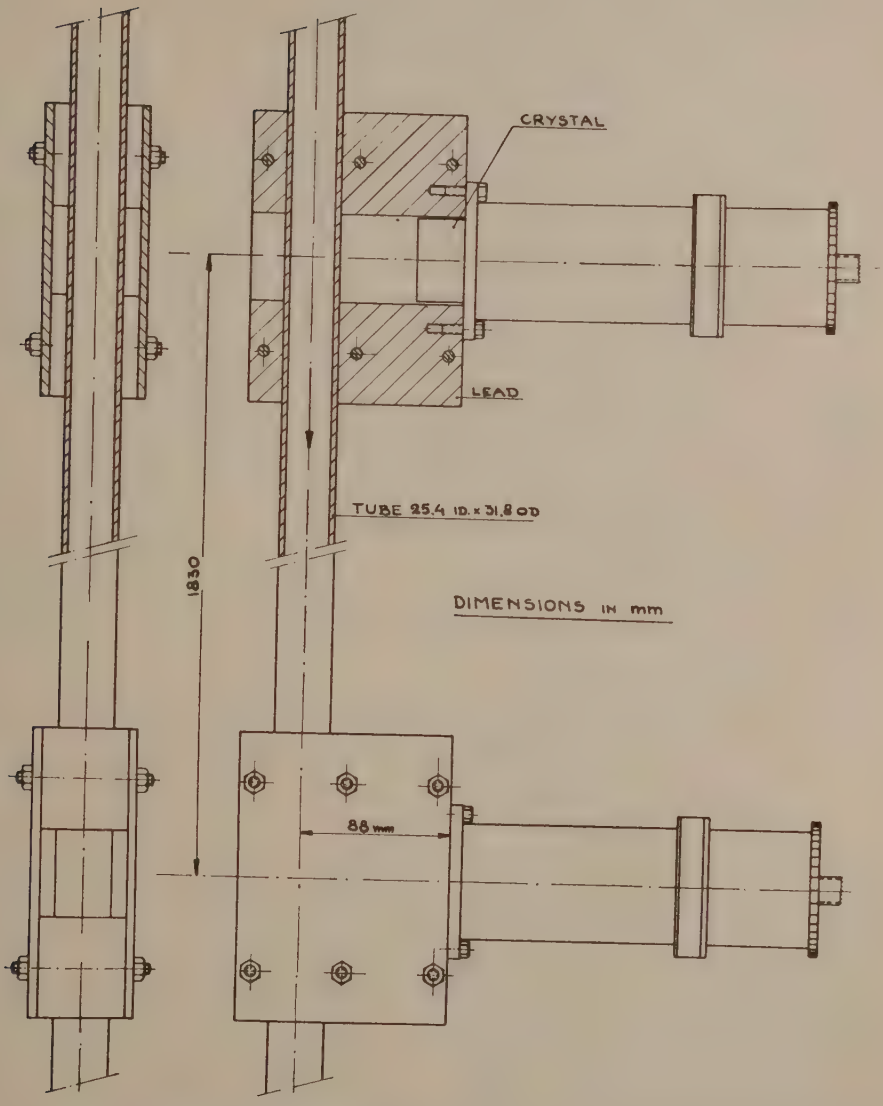

Fig. 1. Mechanical construction of the collimator used for determining the speed of pneumatically transported grain.

After experiments, the activated grains were simply located in the receptacle by means of a monitor and re-used. For health reasons, only a limited number of grains were activated and used.

Figure 4 shows the circuit diagram used.

There is nothing elegant about sections A and B and the only argument in favour of its use is the fact that it works and was the simplest to make in the limited time available. A more elegant solution would be to use a scaling circuit

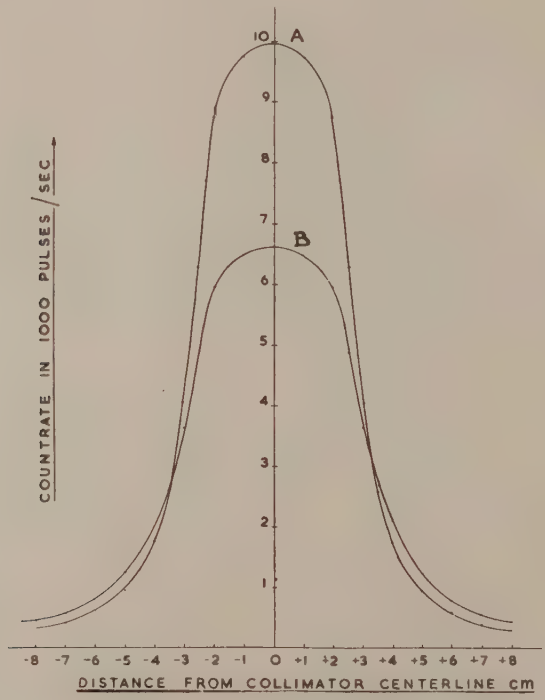

Fig. 2. Counting rate of scintillation counter as function of position of source.

Sections A and B are similar and consist of a 5819 photomultiplier giving positive pulses from the tenth dynode to the amplifier. The IN34 crystal diode catches the anode at a voltage adjustable by means of a potentiometer and hence limits the negative swing on the anode.

The one half of a 12AU7 is used as a cathode follower to drive a non-linear integrating circuit consisting of a IN34 crystal diode and 0.01 μF condenser, the idea being that the charging time constant would be long but the discharging time constant short, so that appreciable voltage buildup across the condenser will occur only if the count rate exceeds a certain value. The voltage across the condenser is amplified and used to trigger a 2D21.

which is reset cyclically so that output pulses are obtained only if the count rate exceeds a certain value determined by the frequency of resetting. Scaling tubes may be used but with the associated driving circuits the complexity would be greater than that of the circuit employed.

An output pulse from A triggers the "on" thyratron 2D21 which applies screen voltage to the 6AC7 gate tube. A pulse from circuit B fires the "off" thyratron which lowers the anode voltage of the 6AC7 gate. Pulses from a 6SL7 twin-T oscillator are fed on to the grid of the gate and from the anode of the gate to a dekatron-scaler with the necessary drivers.

A pulse from A will therefore cause screen voltage to be applied to the gate and cause 2

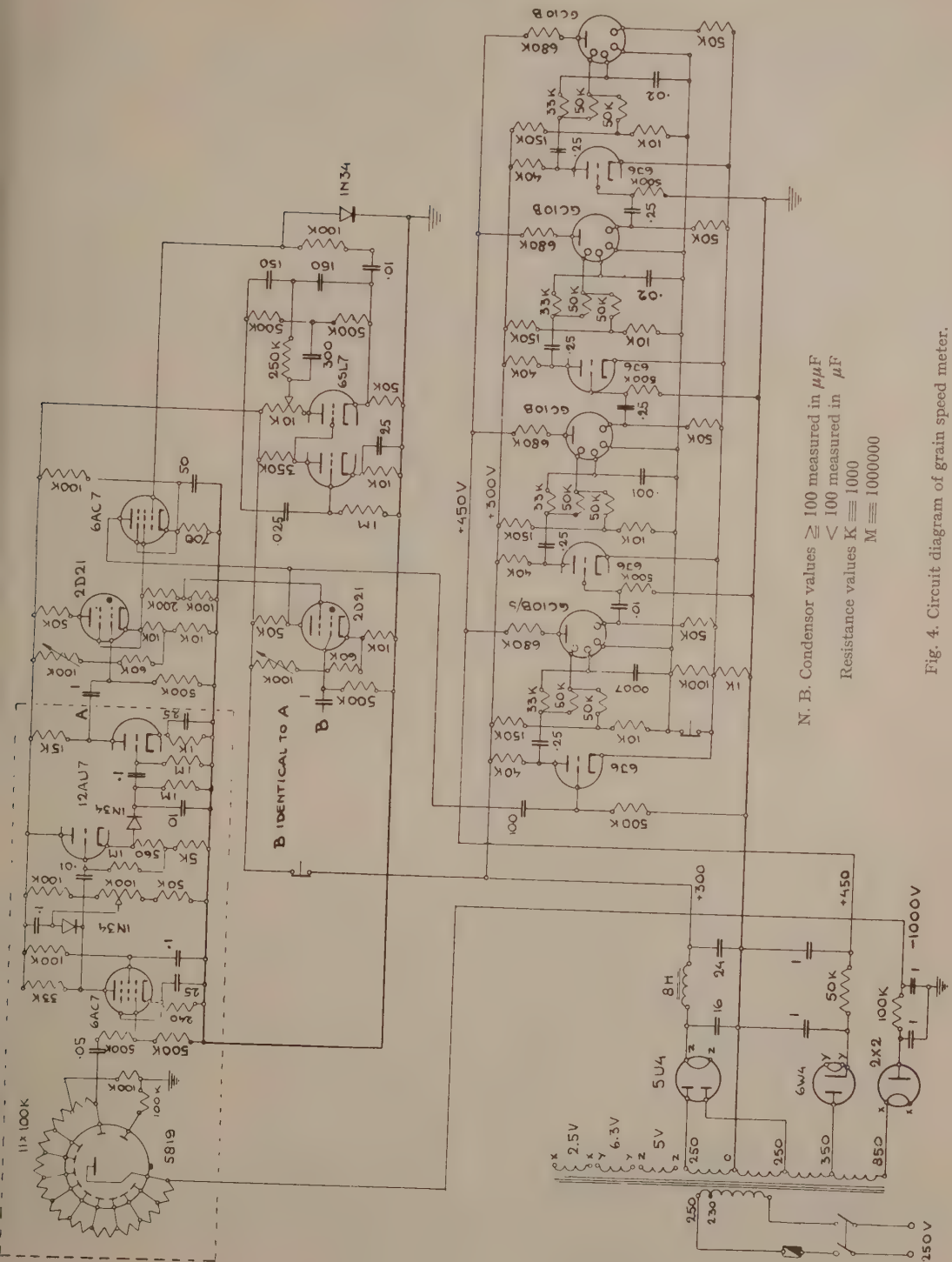

Fig. 4. Circuit diagram of grain speed meter.

kp.p.s. to be fed to the dekatron-scaler. A subsequent pulse from B will fire the "off" thyratron which will then stop the timing pulses from reaching the scaler.

After a reading the circuit is reset by extinguishing both thyratrons and resetting the scaling circuit by means of a pushbutton.

Power supplies are provided for the scaler and the scintillation counters in a fairly compact unit as shown in fig. 4.

The author wishes to thank Mr. Verwey of the Biophysics section for the activation of the grains, Mr. Roux for his help in the construction of the apparatus, and the Council for Scientific and Industrial Research for the facilities granted and permission to publish this paper.

Total number of counts vs. position for a grain speed of 18.3 m/sec.

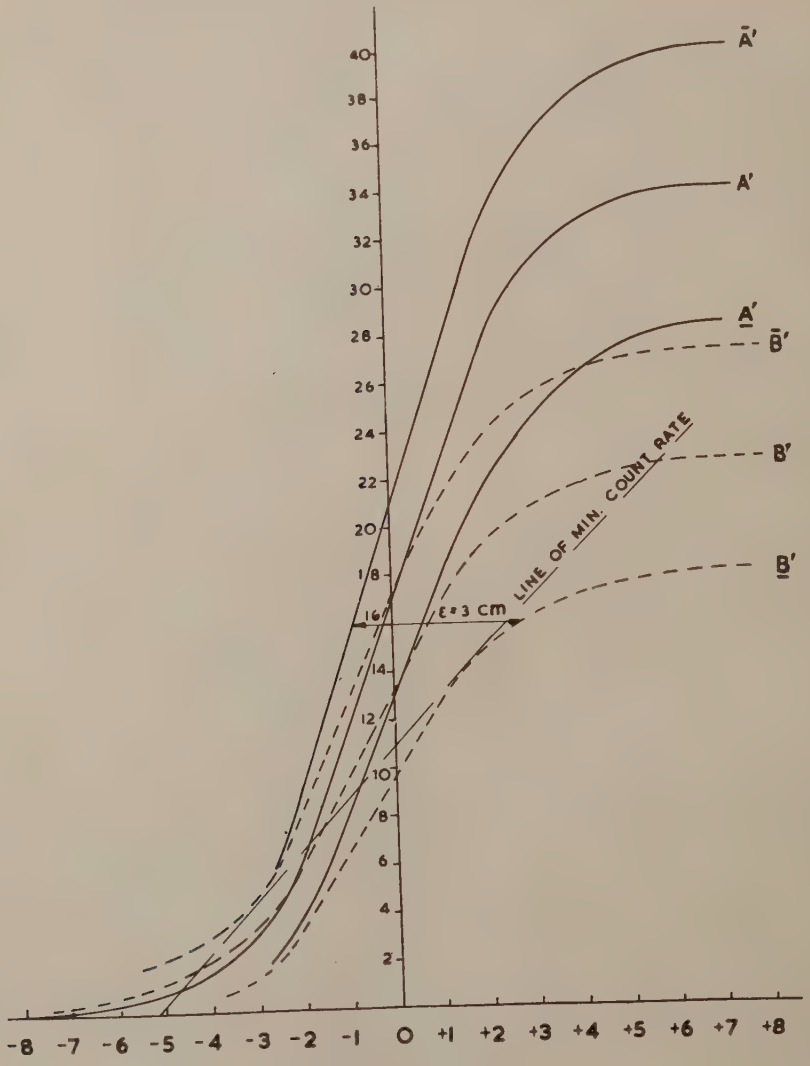

Fig. 3. Position in cm.

NUCLEAR INSTRUMENTS 1 (1957) 71–74; NORTH-HOLLAND PUBLISHING CO. – AMSTERDAM

TEMPERATURE COEFFICIENTS OF SCINTILLATING SYSTEMS †

WILLIAM P. BALL, REX BOOTH and MALCOLM MACGREGOR

University of California Radiation Laboratory Livermore, California

Received 12 November 1956

Temperature coefficients of several photomultiplier tube-scintillator combinations and of photomultiplier tubes separately have been measured over the temperature range from 5° C to 40° C. The coefficients, which are negative, are functions of the temperature. The coefficient for the photo multiplier-scintillator combination is typically — 0.5%/° C which means that temperature regulation is essential for systems which require accurate gain stability.

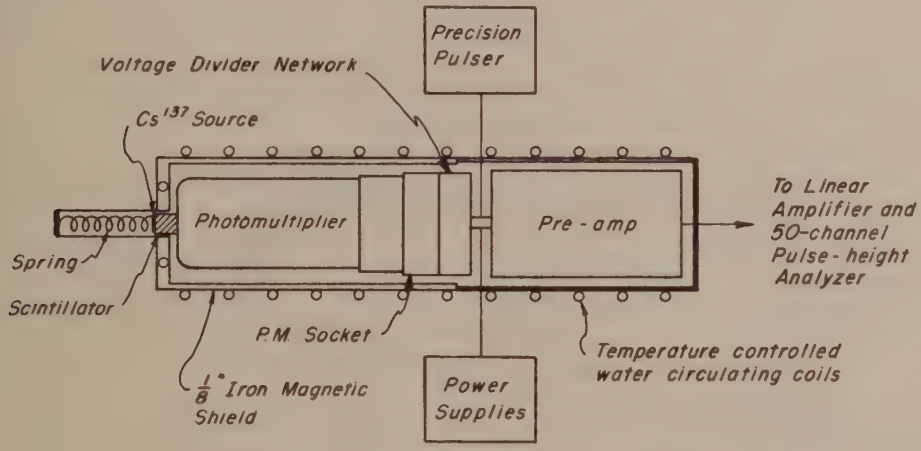

Fig. 1

Introduction

In many applications of electronics, gain stability of the entire system over long periods of time is required. In this regard one factor should not be overlooked is the effect of temperature on the gain of photomultiplier tubes and scintillating materials[1–7]). Of particular interest to physicists and others is the temperature cofficient of the system—photomultiplier tube plus scintillator. Two methods that can be used to eliminate temperature effects are to provide a temperature stabilized environment for the scintillator system[2,9]) or to design compensating electronic circuits[6]). In either case a knowledge of the overall coefficient of the system is necessary in designing an arrangement for a predetermined level of stability.

In the present experiment the temperature

† Work performed under the auspices of the U. S. Atomic Energy Commission.

[1]) L. A. Webb, U. S. Naval Radiological Defense Laboratory, San Francisco, Calif, USNRDL-TR-48, N. S. 081001 (1955).
[2]) J. R. Beyster *et al.*, Phys. Rev. **98** (1955) 1216.
[3]) H. Kallman, AECU-583 (1949) 8.
[4]) S. H. Leibson and J. W. Keller Jr., Phys. Rev. **78** (1950) 305.
[5]) J. A. Dooley and H. Shull, Iowa State College, ISC-497 (1953) 104.
[6]) Herold, Kropp and Stutheit, E. I. du Pont de Nemours & Co., Savanna River Laboratory, DP-47 (1956).
[7]) H. H. Seliger and C. A. Zeigler, Nucleonics **14** (1956) 49.
[8]) R. L. Caldwell, and S. E. Turner, Nucleonics **12** (1954) 47.
[9]) MacGregor, Ball and Booth, Phys. Rev. (submitted).

coefficients of four scintillating systems—photomultiplier tube plus anthracene, stilbene, sodium iodide, and plastic—were determined over the range 5° C to 40° C. As an additional measurement, the temperature coefficient of the photomultiplier tube used with the above scintillators was obtained separately with the use of a light pulser. This permits at least an approximate separation of the temperature coefficient into scintillator and photomultiplier components. And, finally, a series of six RCA 6199 and DuMont 6291 photomultiplier tubes were comcompared as to average temperature coefficients over this range, using the light pulser arrangement.

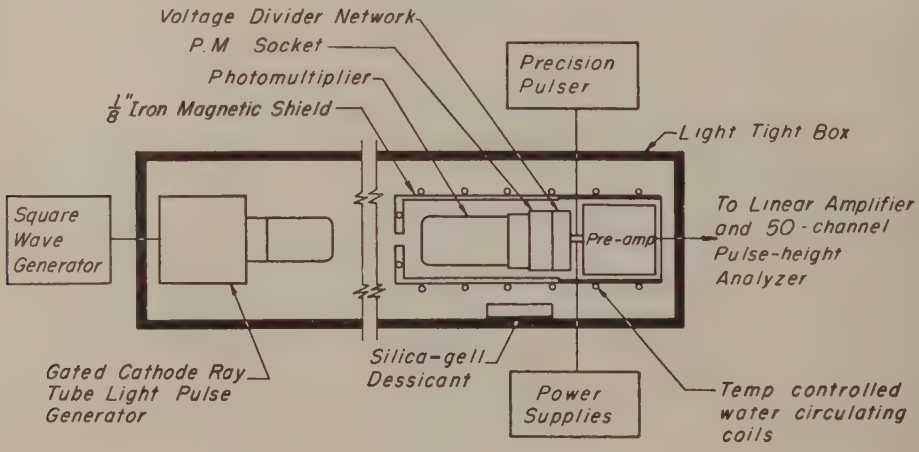

Fig. 2

Experimental Arrangement

The measurement of the system—photomultiplier tube plus scintillator—was accomplished by means of the arrangement shown in fig. 1. The conversion electrons from Cs^{137} were used to produce pulses in the three organic scintillators, and the Cs^{137} gamma rays were used in the case of NaI(Tl). These pulses were observed on a 50 channel differential pulse-height analyzer (PHA). The temperature of the photomultiplier assembly was controlled by means of water flowing through a copper-tubing network surrounding the magnetic shield (see fig. 1). A portable refrigeration system was used to obtain stable water temperatures which were varied in random fashion from 5° C to 50° C. As the temperature of the assembly was changed, the shift in the pulse height was noted on the 50 channel pulse-height analyzer. About an hour was required after each temperature change for the system to come to a steady state. The stability of the amplifier gain was checked by introducing the signal from a precision pulser at the input to the preamplifier and displaying the output of the amplifier on the 50 channel PHA simultaneously with the signal from the Cs^{137} source. The preamplifier exhibited no measurable change in gain over the range of temperatures used in the experiment. A separate measurement, with the photomultiplier tube removed from the temperature-controlled case and connected to the tube base with an extension cord, showed that the tube voltage divider network introduced no temperature effects. Hence the change in pulse height with temperature was attributed solely to the photomultiplier tube and to the scintillator.

The temperature coefficient of the photomultiplier tube alone was measured using the arrangement shown in fig. 2. The scintillator was removed and replaced by a light pulser. This consisted of a gated RCA No. C-73687experimental cathode-ray tube with a P-16 screen which was pulsed with 0.6 microsecond square waves at a repetition rate of 100 per second. The

temperature of the photomultiplier tube was varied, while the temperature of the light generator remained constant.

Results

The pulse-height versus temperature measurements are shown in fig. 3. The same photomultiplier tube was used in all of these measurements. Only one sample of each scintillating material was tested.

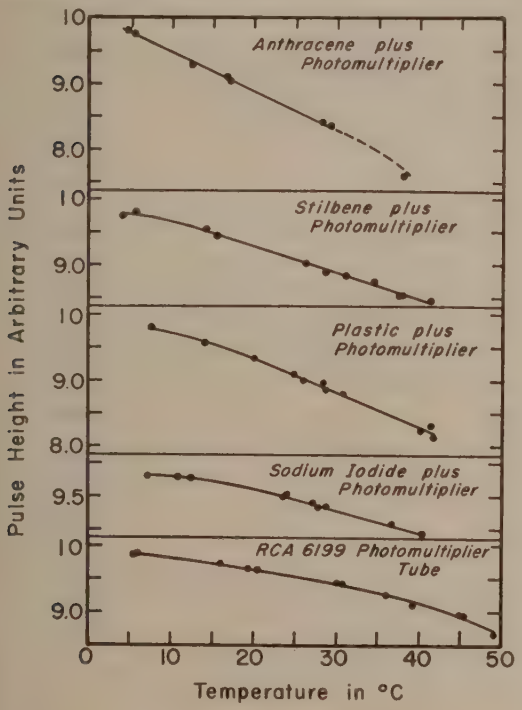

Fig. 3

Three each of the DuMont 6291 and RCA 6199 photomultiplier tubes were tested for average temperature coefficients over the range 5° C to 50° C. The results are as follows:

Tube		Average Coefficient (%/° C)
RCA 6199	No. 1	— 0.42 ± 0.05
	No. 2	— 0.5 ± 0.1
	No. 3	— 0.27 ± 0.03
DuMont 6291	No. 1	— 0.2 ± 0.1
	No. 2	— 0.22 ± 0.1
	No. 3	— 0.28 ± 0.1

Several other points were also noted. Observation of the tube noise as a function of temperature showed that the number of pulses observed on the 50 channel PHA went down by a factor greater than 10 in going from 40° C to 5° C, while the height of the pulses remained substantially constant. The temperature coefficient of the photomultiplier tube was found to be independent of the tube high voltage over the range tested, 650 to 950 volts. No systematic hysteresis effects[1]) were observed in any of the measurements made. At fixed temperatures, no change in pulse height with time after turn-on[8]) was observed.

Discussion

The information of immediate practical interest[6]) is contained in the top four curves of fig. 3. The scatter of the points gives a measure of the uncertainty of the curves. For investigators who are concerned with temperature coefficients *per se*, the bottom curve of fig. 3 may be suitably subtracted from the other curves to give temperature coefficients for the scintillating materials alone. However, a word of caution must be applied in following this procedure. If the temperature coefficient of the photomultiplier system can be attributed to a frequency shift either in the light emitted from the scintillator or in the response characteristics of the photomultiplier tube[7]), then it may not be correct to compare data obtained with a light pulser to data obtained from a scintillator light source. However, the fact that the temperature coefficient thus obtained for sodium iodide (— 0.1 %/° C) agrees well with data obtained by Webb[1]), who measured the temperature coefficient of the scintillating material only, suggests that this method may not be seriously in error. It should be pointed out that since Seliger and Zeigler[7]), using optical filters, obtained a positive temperature coefficient for a series of RCA 5819 and DuMont 6292 photomultiplier tubes, the various experiments are not yet in agreement, and there may be factors entering into the measurements which are not yet properly understood.

The six photomultiplier tubes tested all gave negative temperature coefficients. The values obtained agree well with the value obtained by Webb[1]) (—0.35 ± 0.02/° C), who used a DuMont 6292 photomultiplier tube and a NaI scintillation light source. Herold[6]) obtained temperature coefficients of about —1 %/° C for a series of NaI-photomultiplier tube systems, using both RCA 5819 and DuMont 6292 tubes. A study of these reports together with that of Seliger[7]) indicates that there is no systematic difference, with respect to temperature coefficients, between the RCA and DuMont tubes tested.

NUCLEAR INSTRUMENTS 1 (1957) 75–79; NORTH-HOLLAND PUBLISHING CO. – AMSTERDAM

A VERY FAST PULSE-HEIGHT ANALYSER WITH INDEPENDENT UPTAKE, SORTING AND STORAGE OF INFORMATION

R. V. GÅSSTRÖM†

Physical Laboratory, University of Groningen

Received 26 November 1956

A kicksorter is proposed with an uptake resolution of the order of 10^{-8} s and a mean counting rate without loss of 10^5 pps. The principle is suited for both continuous as well as intermittent sorting and is based on a storage-tube display of the uptake which is scanned for sorting. The read-off information is temporatily stored per channel before it is injected into a large capacity accumulating memory.

Introduction

In particle, quantum and time-of-flight spectrometry the use of pulse-height analysers or kicksorters, as they are popularly called, has been firmly established. Many different types serving satisfactorily various needs are now in use. With the coming of pulsed and high energy accelerators a special need for very fast kicksorters has arisen. Time is at a premium because the exploitation of such apparatuses is expensive. The cost of a run may in some cases exceed many times the cost of the apparatus with which the data is being handled. The duty cycle and yield of pulsed accelerators being low, the information handling equipment should be sufficiently fast to minimize loss of wanted data.

Hutchinson and Scarrott[1]) have given a sorting principle which can be coupled to a memory with a large storage capacity which is efficient and not too bulky. The disadvantage of their apparatus is its long deadtime. Cunningham and Reaves[2]), on the other hand, have shown the practicability of a fast analogue crt memory which can be used for pulse sorting.

The pulse-height analyser proposed in the present paper is very fast and has a memory with a large storage capacity. The author has noticed, when using a phototransistor-crt analyser[3]), the advantages which can be derived from an arrangement where *the display of the pulses for sorting and the sorting itself are processes independent of each other.* Not only is the galvanic connection between the display and sorting electronics advantageously dispensed with, but in the proposed analyser the display and sorting of pulses are also time independent to an extent flexible enough in use. This is of importance when statistically distributed pulses are being analysed. It is possible to increase the time resolution of the display element and to temporarily store analogue information, after which the digital sorting may take place at a slower speed. This should, of course, somewhat exceed the mean rate of the incoming statistically distributed pulses. In some laboratories the periods between intermittent bursts of pulses have been made use of for sorting. The principle proposed here permits a construction suitable for both continuous as well as intermittent aggregation of information.

The Principle

In the proposed analyser the pulses originating from the detecting element are memorized analogically as a pulse-height distribution display on a crt screen (fig. 1). This display

† On leave of absence from University of Helsinki.

[1]) G. W. Hutchinson and G. G. Scarrott, Phil. Mag. **42** (1951) 792.

[2]) G. A. Cunningham, Phys. Rev. **91** (1953) 437; Nat. Bur. of Stand. Report 3258.

[3]) R. V. Gåsström, Physica **22** (1956) 619.

process we shall call the *writing* down of the pulses. The analogue information is then *read* off digitally into different channels by the sorting element. This element may either be a crt storage tube, like Cunningham used, or it may be a camera tube focused on the screen of the writing crt. The beam of the reader sweeps across the pulse-height distribution display and picks up the stored pulses, each sweep forming a channel. The channel width is mainly defined by the beam width if overlapping is prevented. As the reading proceeds the digital information belonging to a given channel is passed on to a temporary store.

In fig. 2 a block diagram of the kicksorter is given. The pulses from the detector are amplified if necessary and shaped, for instance by a delay-line before being applied to the deflection plates of the writer. A count or stop gate should be provided for. A Z-gate intensifies the beam for the duration of the top of the pulse. Synchronization of these operations can be attained by the use of suitable delay-lines at the proper places. Each pulse shifts the beam one step further in the horizontal direction. The distance between the pulses is determined by the resolution of the screen and the speed with which they can be read off into the binary scaler which serves as the temporary store for the pulses of a given channel. There are two such scalers which alternately serve the purpose of a temporary memory or as an adding element used for inserting the pulses of a given channel into the delay-line memory at the proper moment. If no loss of pulses other than that caused by the dead time of the writer can be allowed for, the velocity of the channel sweep is determined in practice by the time resolution of the binary scalers.

The reader element picks up the pulses belonging to a channel and passes them on to an amplifier and an amplitude discriminator. A

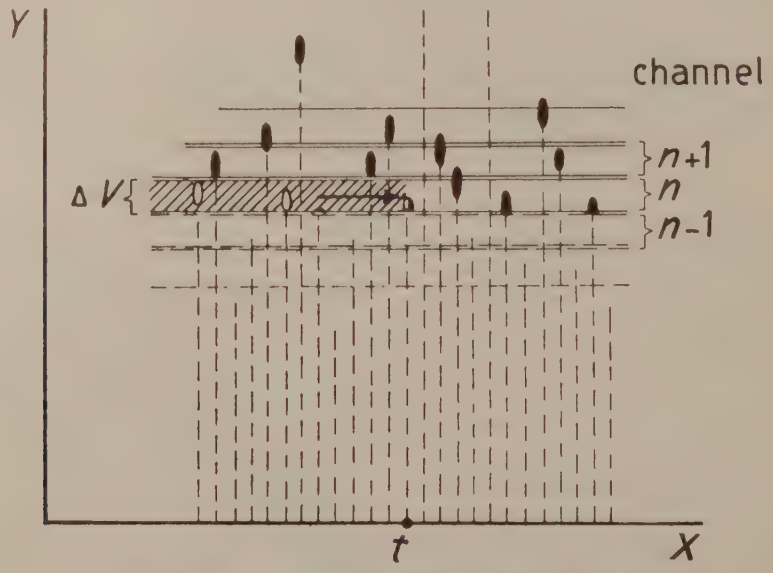

Fig. 1. Schematic diagram of display and sorting elements.

Writer: X deflection takes place stepwise per incoming pulse. Y deflection is proportional to the pulse-height.
Reader: X sweep picks up and erases pulses belonging to a given channel. Y step-voltage determines channel position.

The reader beam width ΔV determines the channel width of analyser. At t the beam is sweeping the n-th channel. It has erased the pulses marked by the white dots. These pulses have been passed on by the pick-up anode to the amplifier unit in order to be discriminated from screen noise and tested for anticoincidence in boundary cases.

delay-line anticoincidence circuit discards pulses which lie on the border of two channels if they have been registered in the previous channel. The pulses are then directed by a flip-flop gate into the correct binary scaler for temporary storage.

The overall synchronization is attended to by the main trigger pair which starts both the bit oscillator and the linear sweep at the beginning of each cycle of the delay-line memory. Bit pulses are fed to the adder in order to reshape the memorized pulses in the delay-line which

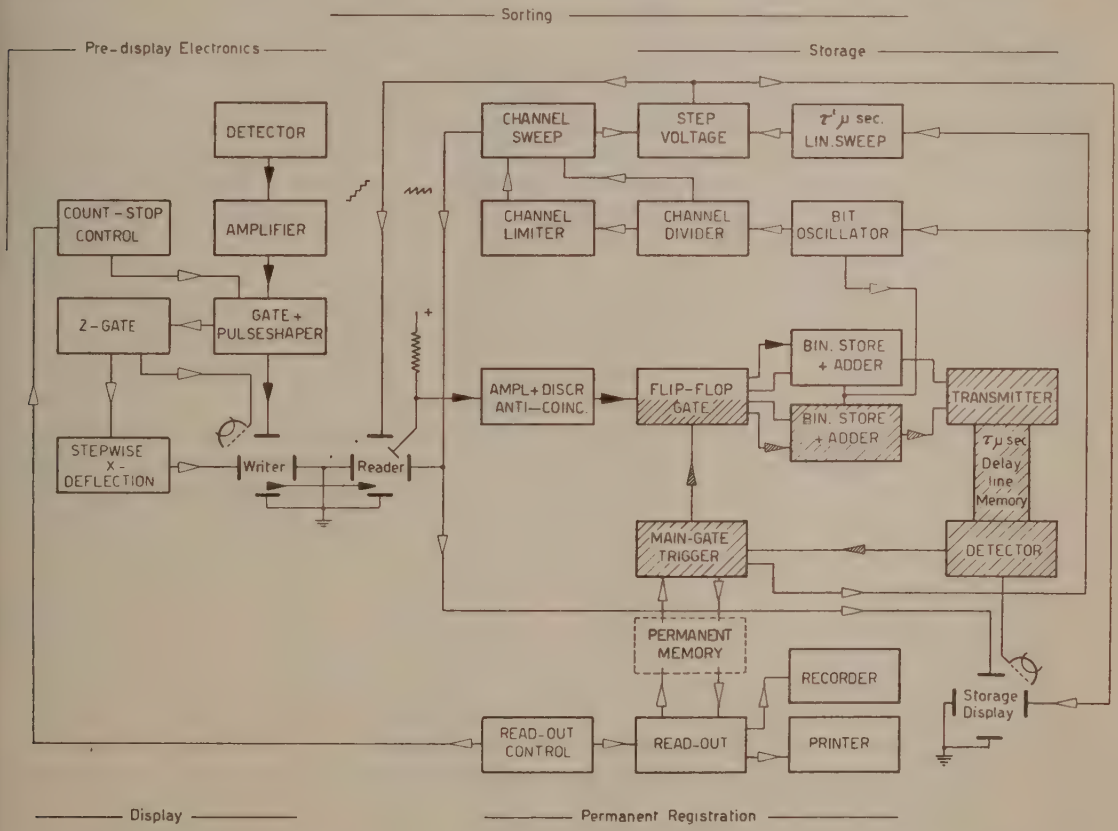

Fig. 2. Block diagram of proposed pulse-height analyser. The black arrows show the path of the pulses as they are being analysed and the shaded arrows show the path of the pulses in the delay-line memory cycle. The blocks of this cycle are shaded.

Simultaneously with this process, the second binary scaler serves as an adding element. The old pulses coming from the delay-line by means of the flip-flop gate and the new pulses stored during the previous sweep are here added and then passed on to the transmitter for injection into the delay-line memory. During the next sweep of the reader the flip-flop gate interchanges the function of storing and addition between the two binary scalers.

may have diffused to some extent. Pulses are also fed from this oscillator to a divider which gives out channel pulses. These pulses start the channel sweep and control the flip-flop gate. In addition, the channel pulses may be directed to a divider which defines the number of complete channels desired.

The channel saw-tooth voltage is combined with a long linear sweep, synchronous with and somewhat shorter than the cycle of the delay-

line, to form a step voltage which shifts the channel sweep of the reader stepwise in the vertical direction.

The continuous display of the accumulated distribution function is accomplished by modulating the intensity of the electron beam while it sweeps over the screen of the storage display crt. The vertical displacement is obtained from the channel sweep and the horizontal displacement from the step-voltage. Thus the channels are placed along the x-axis while the number of counts in each channel is displayed along the y-axis of the crt. For permanent registration the analyser may be stopped and the display either read off or photographed.

In addition the information may also be read out by an automatic printer or recorder to speed up the process. The read-out circuit gets its information from the main gate, which singles out the pulses belonging to a given channel in the order of the channels. The main gate is in turn gated by the read-out mechanism according to the completion of the different functions performed. The read-out circuit transforms the information into a form which is suited for the operation of a paper recorder or a printer. In the figure an additional permanent magnetic memory is shown by dotted lines. If such a memory is used the delay-line cycle may be shorter and a permanent record is obtained at the same time as the accumulation of information proceeds. If the delay-line cycle is made shorter the mean rate of incoming pulses may be increased in the same proportion without affecting the percentage of loss of pulses.

Additional Remarks

As already mentioned, the distribution function aggregated in the delay-line memory may be continuously displayed as in the Hutchinson-Scarrott arrangement, or continuously fed into a permanent memory of larger storage capacity if necessary, or read out and recorded. Some of these features have been realized by Gallagher, Lang and McKibben in their Los Alamos H-S kicksorter[4]). An easily read decimal-coded digital crt-display suited for photographic permanent recording has been developed by Maeder[5]).

If a magnetic storage system can be made to accept pulses at several megacycles per second the delay-line memory could be dispensed with. When data is accumulated during a very costly run a permanent memory is an advantage because the stored data is not affected by power line failures and the like.

It is also possible to use an electrostatic storage tube in place of the delay-line memory. The transmitter and detector would then be superfluous. Instead a transcriber synchronized by the linear sweep and a read-out arrangement would have to be added. An electrostatic storage tube could also take over the storage function of the binary scalers but the operation of addition would require additional electronics.

The above-mentioned Cunningham-Reaves arrangement is suited only for intermittent analysis. But in this case the reading is done with the same deflection system as the writing and therefore the problem of linearity is very much simplified. On the other hand, the camera-tube-crt combination is suited for both continuous as well as intermittent sorting. The light density gradation of the system does not have to be perfect if only the screen does not contain abrupt irregularities. At present an orthicon tube with a lens system seems to be the best solution for a continuous arrangement. If the memory inertia of a vidicon tube could be considerably reduced, the problem of continuous sorting would be greatly simplified. The best solution to this question though would be an electrostatic storage tube in which the writing and reading processes could take place simultaneously.

In conclusion let us consider some numerical values which could be realized with components available at present. As the writer functions independently of the reader the speed of the writing depends only on the pre-writer electronics provided the spot of the pulse top can be

[4]) J. D. Gallagher and J. L. McKibben, Los Alamos Report LA-1917 (1955).

[5]) D. Maeder, Decimal pulse coding storage system (to appear in Helv. Phys. Acta).

memorized on the screen to a degree which is still readable. Cunningham [2] has shown that the resolving time of the uptake of a modern crt or storage tube is of the order of ten millimicroseconds and in the future it may even become better. On the other hand, the mean rate of pulse handling without a loss of pulses after the display depends on the reader and the time needed for a complete cycle of the delay-line memory. Thus, for example, if one hundred pulses are stored side by side on the screen and the channel sweep has a duration of ten microseconds, a one hundred channel analyser would have a maximum mean rate of 100 000 pulses per second. This would mean that the scalers must have a time resolution of 0.1 μsec. in which case the loss of pulses would be exclusively determined by the dead-time of the writer.

It is obvious though that the loss in the sorter is not appreciably increased even if the mean rate increases by a factor of ten. The probability that two pulses statistically spread over the screen would be counted as one is very small. Furthermore this loss is negligible in comparison with that caused by the dead time of the detector and display electronics. This means that statistically distributed pulses could be analysed with a few percents loss at a mean rate of incoming pulses of one million per second. Only very special problems, however, would require such high counting rates.

The storage capacity of a fused quartz delay-line memory can easily be made so large that a one percent statictical error is possible for peak values if the number of channels does not exceed 120[4]). One could at present with the above principle expect to attain an overall linearity of pulse-height analysis of the order of one percent in the case of continuous sorting.

This work has been performed at the Physical Laboratory of the Groningen State University, director Prof. Dr. H. Brinkman, with the support of the Foundation for Fundamental Research of Matter (F.O.M.), subvented by the Netherlands Organization for Pure Research (Z.W.O.).

NUCLEAR INSTRUMENTS 1 (1957) 80–85; NORTH-HOLLAND PUBLISHING CO. – AMSTERDAM

FINE TIME-STRUCTURE OF BEAMS FROM THE BIRMINGHAM PROTON SYNCHROTRON

N. E. BOOTH and G. W. HUTCHINSON

Department of Physics, University of Birmingham

Received 10 December 1956

The radio-frequency time-structure of beams scattered from internal targets in the Birmingham proton synchrotron has been investigated using a delayed self-coincidence technique. The degree of bunching of all the beams commonly used in counter experiments has been investigated and methods of increasing the burst length and destroying the radio-frequency structure are discussed.

1. Introduction

The Birmingham proton synchrotron is capable of accelerating protons to a maximum energy of 1000 MeV[1]). The experiments described in the present paper were performed with protons scattered from various internal targets near the outside or inside of the vacuum box of the synchrotron. Several methods are available for bringing the circulating beam onto a given target.

(a) To force protons of less than full energy onto an outside target at some time during the acceleration cycle, the R.F. accelerating voltage may be switched from the normal variable frequency to a fixed frequency, previously adjusted to the appropriate value. The fixed R.F. increases the rate of gain of energy of the circulating beam and drives it towards the outside of the vacuum box where it may be intercepted by the target.

(b) A similar method may be used at full energy. For $\approx$ 200 msec. before the end of the acceleration cycle, but while the magnetic field is still rising, the R.F. is locked to the appropriate fixed frequency, displacing the beam toward the outside of the vacuum box. Soon after the magnetic field reaches its maximum value the fixed frequency voltage is switched off, and the circulating protons continue to spiral outwards under the influence of the decreasing magnetic field. The protons start to arrive at the target without appreciable delay and while the magnetic field is changing slowly. By this means the burst of scattered particles from the target may be made as long as 30 msec.

(c) If the R.F. is merely switched off at peak magnetic field the burst occurs at a more steeply falling part of the magnetic field cycle and the burst length is only 5–10 msec.

(d) The circulating beam may be made to strike a target near the inside of the vacuum box by merely switching off the R.F. during the acceleration cycle. In practice this system gives a burst length of $\approx$ 5 msec.

(e) A scheme proposed by Goldsack[2]) and now extensively used in this laboratory uses both an outside and an inside target, thus providing two beams for experimental use simultaneously. A polythene wire target of 2 mm square cross section near the outside of the vacuum box is used in conjunction with a Be block target on the inside. The R.F. is switched to fixed frequency and the beam is driven onto the wire target. After several traversals of the wire target protons have lost sufficient energy to build up an amplitude of betatron oscillation

[1]) P. B. Moon, L. Riddiford and J. L. Symonds, Proc. Roy. Soc. A **230** (1955) 204.

[2]) S. J. Goldsack, Nuclear Instruments **1** (1957) 90.

large enough to cause them to strike the inside target.

For time-of-flight experiments it is important to have short intense bursts of particles. However, for most counter experiments it is desirable to have a high circulating beam intensity but to have the scattered beam extend with uniform intensity over as long a period as possible. If there are short intervals in the length of the scattered beam during which the intensity is much higher than the average over the length of the burst, pulse pile-up and dead time effects may have to be considered and these are sometimes difficult to estimate. It is therefore advisable to have kowledge of the time structure of an experimental beam. The gross time structure can be obtained from oscilloscope traces of the counter outputs. The present paper is mainly concerned with the structure on a finer time scale, namely that corresponding to the period of the R.F.

2. Experimental Arrangement

Two photomultipliers with plastic scintillators were placed outside the vacuum box and as near as convenient to the scattering target. A block diagram for one of the multipliers is shown in fig. 1. The signals from each of the

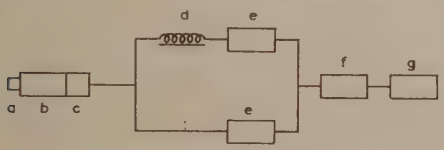

Fig. 1. Block diagram of the electronics.

a — plastic scintillator
b — photomultiplier
c — head amplifier
d — delay cable
e — 100 Mc/s amplifiers
f — coincidence mixer
g — amplifier and scaler

photomultipliers were fed to two 100 Mc/s bandwidth amplifiers via lengths of 91Ω coaxial cable. The limited outputs of the amplifiers were mixed in double coincidence circuits. For one of the counters, which we shall call the beam counter, the relative delay, d, could be varied over a wide range and the resolving time of the coincidence circuit was $\approx 5 \times 10^{-9}$ sec. Thus the scaler connected to the output of the coincidence circuit recorded the coincidence rate between photomultiplier pulses occuring at time t and at a time $t + d$. The other counter was used as a monitor of beam intensity. The relative delay was set equal to one period of the R.F. and the coincidence resolving time was $\approx 3 \times 10^{-8}$ sec. This method of monitoring is more satisfactory than integrating the beam intensity, because the number of counts recorded per burst in both the beam counter and the monitor counter at a given delay have a similar non-linear dependence upon beam intensity and upon the gross time-structure of the burst.

3. Measurements

The measurements performed with various scattered beams, and described below, are divided into three sections: 1) full energy beams from an outside target; 2) beams of less than full energy, produced by driving the circulating beam onto an outside target; and 3) beams produced by the Goldsack two target method.

1 FULL ENERGY BEAMS (methods (b) and (c))

No R.F. fine structure is expected for full energy beams as in both methods (b) and (c) the R.F. is switched off several milliseconds before the circulating beam reaches the target radius.

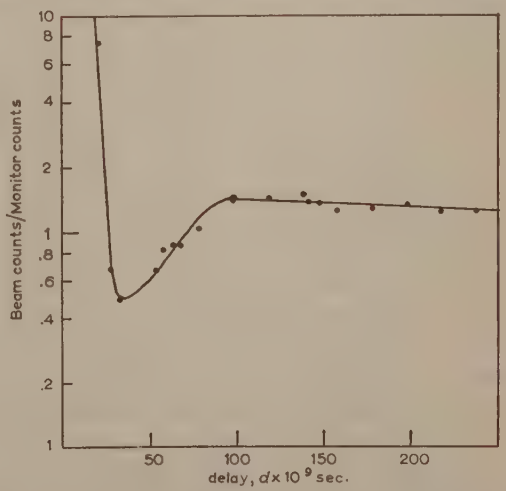

Fig. 2. Delayed coincidence rate as a function of delay time for the full-energy beam obtained by switching off the R.F. voltage at peak magnetic field.

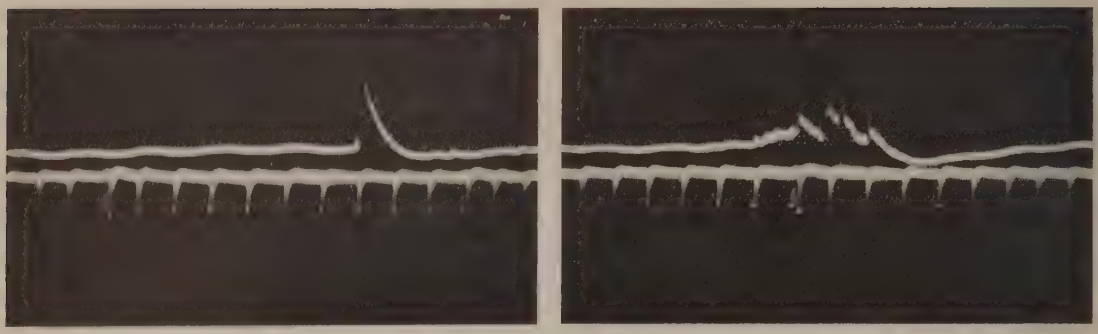

Fig. 3. Scintillator signals.
(a) R.F. voltage switched off at peak magnetic field. (b) Circulating beam driven out at full energy. The calibration marks are 10 msec apart.

This time is long compared with the expected debunching time ($\approx$ 1 synchrotron oscillation period). Therefore we should expect the graphs of delayed coincidence rate versus delay to be flat for time intervals small compared with the duration of any gross irregularities in the burst of scattered particles. Fig. 2, which gives the graph for the fall out beam (method (c)), shows this to be true, except for two features which are mainly instrumental. The first is the marked drop between delays of about 20×10^{-9} sec and 100×10^{-9} sec. At delays less than 20×10^{-9} sec self-coincident counts are recorded. During the period up to 100×10^{-9} sec after the leading edge of a scintillator pulse coincidences are detected with decreased efficiency. This is probably because large unclipped scintillator pulses can block off the 100 Mc/s amplifiers for periods of this order. The second feature, namely the finite negative slope of the curve at longer delays, is also mainly instrumental. Increasing the length of delay cable, especially if more cable interconnections are used, produces a deterioration of the pulse shape. The most important result of this is a decrease in the width of the resolution curve and a corresponding decrease in its area. Of course any longer term variation in scattered beam intensity (whether periodic or not) during the length of the burst would also give a negative slope to the curve of fig. 2.

Similar results were obtained for the driven-out beam (method (b)), except that the ordinate scale was reduced by a factor of more than 20, corresponding to an increase in burst length of $\approx$ 5 times. Fig. 3 shows oscilloscope traces for the two cases obtained by integrating one of the scintillator outputs with a time constant of $\approx$ 100 microseconds.

2 BEAMS OF LESS THAN FULL ENERGY (methods (a) and (d))

When the circulating beam is driven onto an outside target at reduced energies, the fixed R.F. voltage is still on during the time the beam is striking the target. Thus, we expect the scattered beam to exhibit a fluctuation in intensity with the same period as the R.F. Fig. 4 shows the results obtained for a fixed R.F. of 8.76 Mc/s (period 114×10^{-9} sec), corresponding to a circulating beam energy at the target radius of about 700 MeV. The drop in height of the later peaks is mainly due to attenuation in the delay cables, as is their small decrease in width with respect to the first peak. A variation in intensity with a period of $\approx$ 10 R.F. periods could also contribute to the drop in peak height, but no evidence was found for this. The paralysis period of fig. 2 is again evident in the region $10\text{–}60 \times 10^{-9}$ sec. It is possible in principle to work back from the peaks of fig. 4 and the resolution curve (shown in the inset) to find the

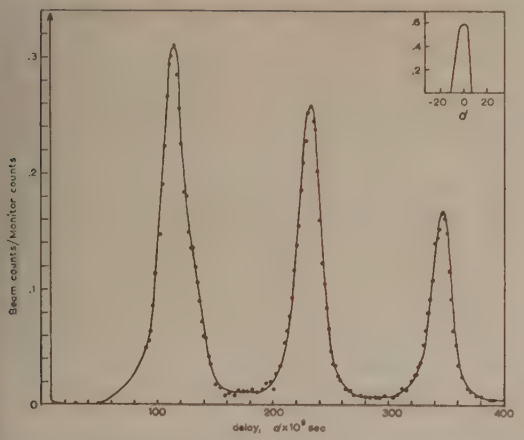

Fig. 4. R.F. structure of scattered beam obtained by driving 700 MeV circulating beam to outside carbon block target. The period of the fixed R.F. is 114×10^{-9} sec. The inset shows the resolution curve obtained with reduced beam intensity. The full-width at half-maximum is 12.6×10^{-9} sec.

R.F. structure of the scattered beam intensity as a function of time.

Let $F(d)$ be one of the observed peaks, and $R(t)$ the resolution curve. Then, if $f(t)$ is the function representing the variation of beam intensity with time, we have

$$F(d) = \int_{-\infty}^{\infty} f(t - d)\,\delta t \int_{-\infty}^{\infty} f(v)\, R(t - v)\,\delta v. \qquad (1)$$

The procedure is to determine the moments of the function $f(t - d)$ from the data, and then, assuming a reasonable form for $f(t - d)$ with arbitrary parameters, choose the parameters to give the observed moments. The first moment is

$$\bar{d} = \int_{-\infty}^{\infty} dF(d)\,\delta d \Big/ \int_{-\infty}^{\infty} F(d)\,\delta d. \qquad (2)$$

Replacing

$$u = t - d \quad \text{and} \quad z = u + d - v$$

we have

$$\bar{d} = \left\{ \int_{-\infty}^{\infty} \delta v \int_{-\infty}^{\infty} \delta u \int_{-\infty}^{\infty} \delta z f(v) f(u) R(z) [v - u + z] \right\} \Big/$$

$$\left\{ \int_{-\infty}^{\infty} \delta v \int_{-\infty}^{\infty} \delta u \int_{-\infty}^{\infty} \delta z f(v) f(u) R(z) \right.$$

$$= \bar{v} - \bar{u} + \bar{z}.$$

Since $\bar{v} = \bar{u}$, we have $\bar{z} = \bar{d}$. This relationship tells us nothing about $f(u)$, but indicates an easy method of calculating higher moments. Taking $\Delta d = d - \bar{d}$, $\Delta v = v - \bar{v}$, etc., so that

$$\Delta d = \Delta v - \Delta u + \Delta z,$$

we have

$$\overline{(\Delta d)^2} = \overline{(\Delta v - \Delta u + \Delta z)^2}$$

$$= \overline{(\Delta v)^2} + \overline{(\Delta u)^2} - 2\,\overline{\Delta v}\,\overline{\Delta u} + 2\,\overline{\Delta v}\,\overline{\Delta z}$$

$$- 2\,\overline{\Delta u}\,\Delta z + \overline{(\Delta z)^2}$$

$$= 2\,\overline{(\Delta u)^2} + \overline{(\Delta z)^2}, \text{ since } \overline{\Delta v} = \overline{\Delta u} = \overline{\Delta z} = 0. \qquad (3)$$

Thus, the second moment of u is given by

$$\sigma_u^2 = \tfrac{1}{2}\,(\sigma_d^2 - \sigma_z^2). \qquad (4)$$

Higher moments may also be calculated in order to determine $f(u)$ to any degree of accuracy.

The second moments of the peaks of fig. 4 and of the resolution curve, taking into account its dependence upon the length of delay cable, were calculated, and gave an average value of

$$\sigma_u = (7.8 \pm 0.8) \times 10^{-9} \text{ sec.}$$

Assuming the beam function to be square, its full width is $2\sqrt{3}\,\sigma_u$ or 27×10^{-9} sec. If the beam function is assumed to be of Gaussian form, $f(u) \approx \exp(-u^2/2\sigma_u^2)$, then σ_u is as given above.

If the functions F, f and R are all assumed to be Gaussian[3], the peaks of fig. 4 and the resolution curve may be analysed graphically to give their Gaussian parameters. The average values obtained are then $\sigma_z = (4.7 \pm 0.4) \times 10^{-9}$ sec and $\sigma_d = (11.5 \pm 1.0) \times 10^{-9}$ sec, giving $\sigma_u = (7.4 \pm 1.0) \times 10^{-9}$ sec. This agrees well with the σ_u calculated by the more general method.

We may take $2\sigma_u$ as a measure of the time in each R.F. cycle during which the outside edge of the circulating beam is striking the target. This is about two thirds of the width of the peaks of fig. 4 and constitutes 14 % of the R.F. period, or about 50° of arc of the vacuum box.

The peak-to-valley ratio and the width of the peaks of fig. 4 are dependent upon good operation of the R.F. accelerating voltage, particularly in the region where the switch-over occurs from the variable frequency to the fixed frequency. Under the same experimental conditions as for

[3]) R. Madey, K. C. Bandtel and W. J. Frank, Rev. Sci. Inst. 25 (1954) 537.

fig. 4 but on a day when the R.F. voltage dropped markedly in amplitude just before switch-over, the peak-to-valley ratio deteriorated from about 30:1 for fig. 4 to 2:1 and the width of the peaks increased by about a factor of 2.

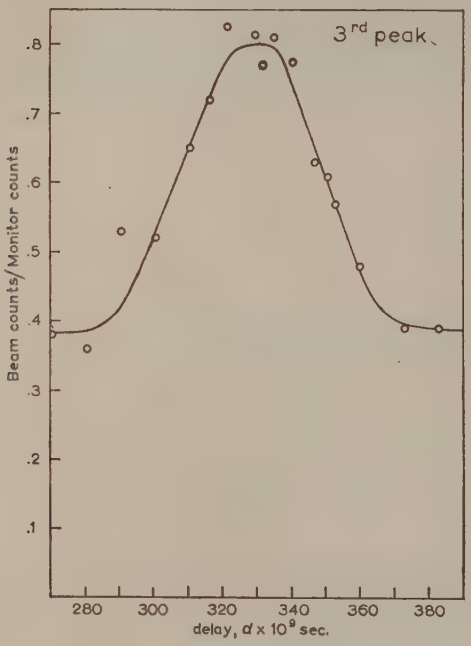

Fig. 5. R.F. structure from outside target obtained by switching to fixed frequency late in the acceleration cycle. This particular time of switch-over produces the longest burst duration ($\approx$ 80 msec).

In practice the R.F. voltage always slowly drops in amplitude towards the end of the acceleration cycle. This has the effect of increasing the azimuthal extent of the circulating beam. Fig. 5 shows the result obtained when the R.F. was switched to fixed frequency late in the cycle. The peak-to-valley ratio is only 2:1 and the width ($2\sigma_u$) is $\approx 26 \times 10^{-9}$ sec or 85° of arc.

Beams scattered from an inside target produced by switching off the R.F. while the magnetic field is still rising (method (d)) are infrequently used because of the advantages of the two-target method. They would not be expected to show any R.F. structure.

3 BEAMS PRODUCED BY THE TWO TARGET METHOD (method (e))

In the experiments performed with the two target system using the polythene wire target near the outside and a Be block target near the inside of the vacuum box the fixed R.F. was still on while the circulating beam was striking the target. No R.F. structure is expected in beams scattered from the inside target. R.F. structure in beams scattered from the outside target would be expected only if coherence is not lost during multiple traversals of the target. We found in fact that coherence was destroyed and that beams scattered from both targets were free from R.F. structure. The energy loss per target traversal is about 400 keV while the energy gain from the R.F. per revolution is at most only 200 eV.

A thin target technique has also been used at Berkeley[4]), but in this case the energy loss per traversal of the target (0.0001" of rubber hydrochloride) was much less than the energy gain from the R.F. By use of a "Clipper electrode" which removes from the circulating beam particles having large oscillations, the Berkeley workers found it was possible to enhance the R.F. structure of the scattered beam.

4. Conclusions

If the R.F. is on while the circulating beam is striking the target, scattered beams exhibit R.F. structure. This offers the possibility of certain time-of-flight experiments. For other types of counter experiments using these beams it is obvious that coincidence circuit resolving times need be no faster than 5×10^{-8} sec because to record more than one coincidence during a single R.F. peak would require a resolving time of $< 5 \times 10^{-9}$ sec and a corresponding scaler resolution. Scaler dead times should be less than 10^{-7} sec so that particles scattered in successive R.F. cycles can be recorded.

If the R.F. is off while the circulating beam is striking the target, there is no R.F. structure in

[4]) H. G. Heard (unpublished), UCRL-3428 (1956).

scattered beams. Higher counting rates per burst may be tolerated when the burst occurs during the slowly changing part of the magnet cycle because the increase in burst length reduces the mean counting rate within the burst.

The two target technique may be used to give maximum burst lengths free from R.F. structure from both inside and outside targets simultaneously. It is therefore very suitable for most counter experiments.

Acknowledgments

We wish to express our thanks to Dr. R. H. Dalitz for discussions about the analysis of the results. One of us (N.E.B.) wishes to thank Imperial Oil Limited for the award of a Graduate Research Fellowship.

NUCLEAR INSTRUMENTS 1 (1957) 86–89; NORTH-HOLLAND PUBLISHING CO. – AMSTERDAM

A TARGET BOX FOR BOMBARDMENT OF CF_4 IN GASEOUS OR SOLID FORM

P. B. TREACY and N. F. BOWKETT

Research School of Physical Sciences, The Australian National University, Canberra

Received 12 November 1956

The construction and operation is described of a target box in which CF_4, either in gaseous or solid form, can be bombarded by protons and the angular distribution of soft (19 (keV) radiation emitted in the process $F^{19}(p.p'\gamma)$ observed. Examples are given of pulse spectra obtained from solid CF_4 and from a conventional target of CaF_2.

Introduction

In the course of studies of extranuclear effects in the nuclear reaction $F^{19}(p,p')F^{19}$ * (197 keV level)[1]) it became necessary to use a gas target, and for this purpose CF_4 was chosen because of certain desirable chemical properties†. In these experiments protons of 873 keV from the Canberra 1.2 MeV H.T. set were used, and the angular distribution of the 197 keV radiation studied. The effect of the presence of a uniform magnetic field applied parallel to the beam was also observed. It was later desired to use a solid CF_4 target under similar conditions, and the gas target was modified for this purpose.

Experimental Details

Fig. 1 shows an elevation of the target arrangement in "exploded" view. The parts shown separately at top and bottom are relevant to the solid CF_4 target (see below). The beam enters the box through a $^3/_{16}$ in. hole in a thin vacuum-tight foil of nickel, of stopping power about 100 keV for 1 MeV protons. This foil is sandwiched between two O-rings spring-loaded together, and is cemented in position with a thin cement of glyptal. The gas chamber is a brass cylinder of vertical axis and $^1/_2$ in. diameter, hard soldered to a brass plate. Gas enters at the base from a separate filling system. With this design it is possible to detect the 197 keV radiation without preferential absorption, to angles greater than 90° either side of the forward direction. The target box is wholly insulated from the beam tube by an ebonite plate held in contact with the beam tube by a brass and steel screw. As is shown in fig. 1, with the screw in place, the beam tube comprises a continuous steel surface which may become the core of the magnet. The whole target assembly fits centrally between the $1^1/_2$ in. magnet poles. It contains no magnetic material except for the negligible mass of the nickel foil.

For observing radiation from solid CF_4 (freezing point —185° C) the attachments shown in fig. 1 above and below the target are screwed to it using O-ring seals. The upper piece is a liquid N_2 reservoir with a solid $^1/_{16}$ in. thick copper target attached to its base. The tube of the reservoir is made of thin stainless steel, polished on its outside surface. This sits in the vacuum as shown and is thermally insulated by a perspex ring. Round the top is a water jacket whose purpose is to prevent freezing of the vacuum seals. The bottom attachment contains a sliding brass valve, which may be pushed up to seal off the beam entry port during filling of the chamber prior to freezing. This attachment need not be used when a nickel foil is in place, and in fact without it the vapour pressure of frozen CF_4 at liquid N_2 temperature is a little high for smooth operation of the H.T. set.

[1]) P. B. Treacy, Nuclear Physics 2 (1956/57) 239.

† Details of experimental results and their interpretation will be published elsewhere.

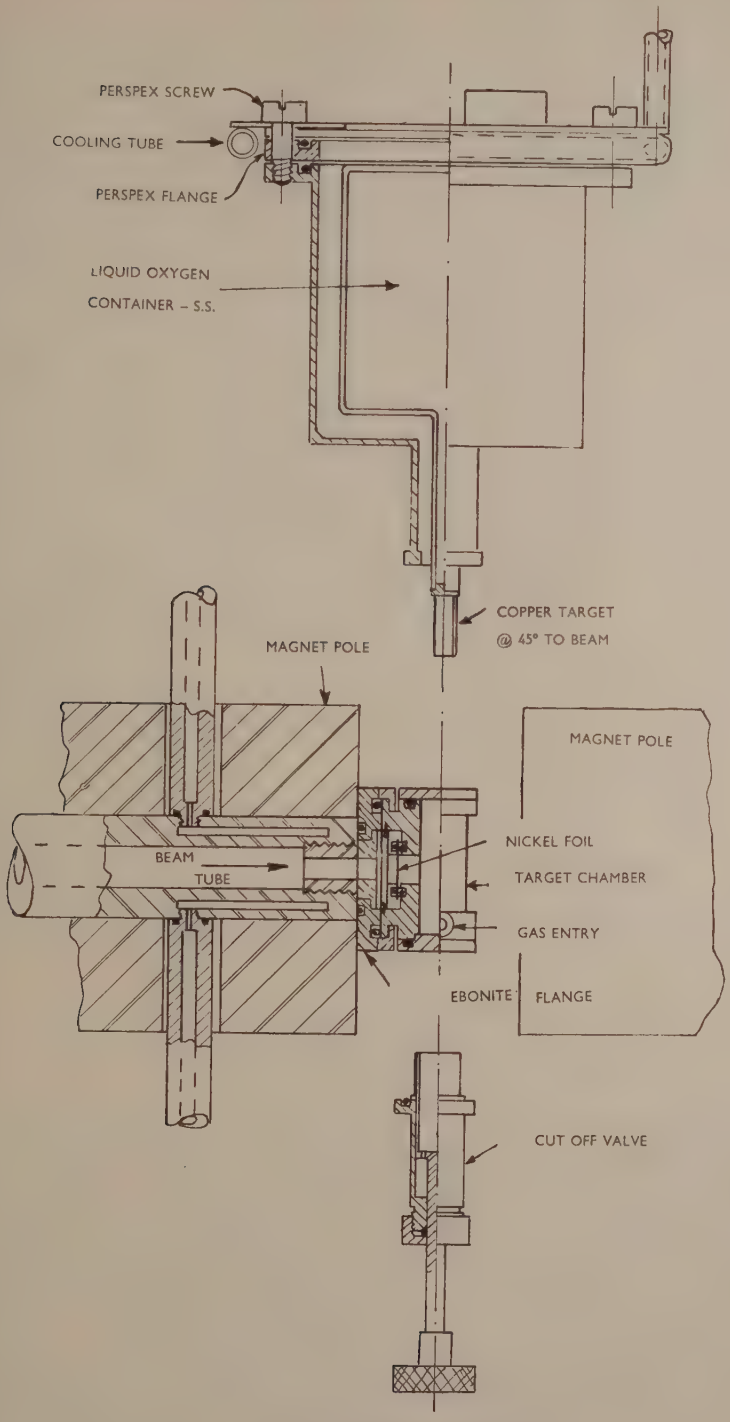

REFRIGERATED GAS TARGET ASSEMBLY

Fig. 1. Elevation view of target box and attachments

Operation

The gas target was operated at a pressure of 2.5 cm Hg. After some hours' use with a beam of 1 μA at 980 keV, the foil distorted slightly but did not appear to change in thickness. It was not found necessary to cool the target box under these conditions.

The thickness of the frozen target was determined by calculating the surface area of so melting of the target material (which would require a rise of 11° C) could be discounted.

The main disadvantage of the target assembly was undoubtedly its massiveness. In fig. 2 are shown the pulse spectra obtained with a scintillation counter and 1" diameter × $^1/_8$ in. NaI(Tl) crystal from solid CF_4, from a "blank", and also from a target of CaF_2 in a different target arrangement of small mass. The curves are

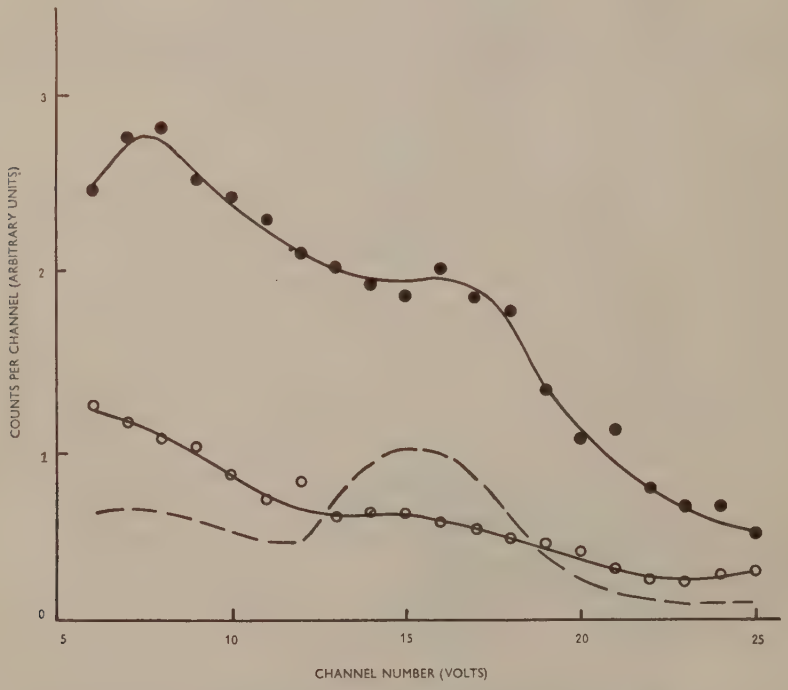

Fig. 2. Typical pulse spectra from $F^{19}(p,p'\gamma)$ using solid CF_4 (full circles) "blank" (open circles) and a CaF_2 target (dotted curve)

"cold" inner surfaces assuming uniform adherence of CF_4 to these. The width of the 873 keV proton resonance in F^{19} was used to confirm the approximate correctness of the estimate. There was no apparent loss of yield throughout several hours' run. This is not surprising when one remembers that the surface layer of CF_4 (about 50 keV for a filling pressure of 1 cm Hg) was of negligible thickness as seen by protons of 1 MeV. Furthermore, the temperature gradient produced in the $^1/_{16}$ in. copper target backing would certainly not be greater than about 2° C normalized to equal charges collected at the target. The effect of scattered 6–7 MeV radiation is evident. The "blank" run was obtained by raising the copper target above the beam, and filling and freezing as usual. This showed the presence of some 10% of contamination, which was attributed to fluorine contamination in the beam tube of the H.T. set.

An examination of fig. 2 shows that it was very difficult to estimate the area under the peak. Spectra were here obtained from radiation observed by transmission through the target

backing set at 45° to the beam. By comparison the spectra obtained from CF_4 gas targets were considerably better, and, even with the magnet poles in position, one could judge the background reasonably well. It was fortunately not necessary to attempt a run on solid CF_4 with the magnet, as here very poor experimental accuracy was obtainable.

We are very grateful to Messrs. J. Kalmar and W. H. Owen for technical assistance. The CF_4 gas was made available by Dr. E. G. Muirhead of Melbourne University.

NUCLEAR INSTRUMENTS 1 (1957) 90–91; NORTH-HOLLAND PUBLISHING CO. – AMSTERDAM

TWO TARGET OPERATION OF A PROTON–SYNCHROTRON

S. J. GOLDSACK

Department of Physics, University of Birmingham

Received 10 December 1956

Introduction

The purpose of the present note is to describe a method of operating targets in a proton synchrotron which offers certain advantages in respect of the efficiency of operation and of the duration of the burst of scattered particles.

This method consists of placing two targets in the vacuum chamber, one close to the inside edge and one close to the outside edge of the region of stable acceleration. These may be in different parts of the machine and the beam from each may be used separately.

The following discussion refers especially to the Birmingham proton synchrotron[1]) but most of the remarks should apply equally to the machines at Berkeley, at Brookhaven, and in the U.S.S.R., and to electron synchrotrons.

Normal Target Operation

To understand the operation of the system it is necessary first to discuss the behaviour of the beam when it strikes targets of the two types in normal operation.

(*a*) THE INSIDE TARGET

A beam can be made to spiral inwards at any moment of the acceleration cycle by switching off the radio-frequency accelerating voltage. The inward spiralling is very slow, about 10^{-4} cms/revolution in the Birmingham synchrotron. If a given particle is initially in a state of oscillation about its mean orbit, its successive points of maximum inward excursion drift very slowly inwards and precess round the machine. The particle therefore first meets the surface of the target close to an antinode in the inward direction. This contact with the target removes some energy from the particle whose mean orbit therefore moves inwards discontinuously, the particle proceeding with a recuced amplitude of oscillation[2]). Further contacts with the target further decrease the amplitude of oscillation until the mean orbit reaches the target radius. After this the next revolution must bring a complete encounter with the body of the target, and the particle will usually emerge with insufficient energy to pass again round the magnet. The characteristic of this case is that the betatron oscillations die out during the first contacts with the targets.

The loss of a given particle from the beam takes place in a very short time once contact with the target is established, but the burst of particles on the target may last a few milliseconds due to the finite size of the beam.

(*b*) THE OUTSIDE TARGET

In this case beam may be directed onto the target by switching off the radio frequency near the peak of the magnetic field, when the beam spirals out under the influence of the decreasing field. Alternatively the radio-frequency may be switched to constant frequency at an earlier point in the cycle when the beam spirals out to maintain synchronous acceleration. Again the rate of spiralling is very small, and by switching to constant frequency a little before peak field it

[1]) P. B. Moon, L. Riddiford and J. L. Symonds, Proc. Roy. Soc. A **230** (1955) 204.

[2]) This behaviour of the inside target was pointed out by McMillan. (E. D. McMillan, Rev. Sci. Instr. **22** (1951) 117.) and forms an essential part of the operation of the extraction mechanism at the Brookhaven Cosmotron (O. Piccioni, D. Clark, R. Cool, G. Friedlander, and D. Kassner. Rev. Sci. Instr. **26** (1955) 232).

may be arranged that the particles begin to strike the target with the magnetic field decreasing only very slowly. In this way bursts have been achieved of duration 80 msecs.

We now consider the details of the behaviour of a given particle as it spirals outwards and touches the target. The first encounter is again very close to an antinode but in the outward direction. The loss of energy moves the mean orbit inwards away from the particle, so that the particle proceeds with increased amplitude of oscillation but with the same outward excursion as before. Several contacts on the target may be necessary to remove enough energy to return the mean orbit to the middle of the vacuum chamber. The particle is now in large oscillation between an outside limit close to the target radius and an inside limit close to the inside wall of the box, and the final fate of the particle will be a collision with the obstruction extending furthest from the inside wall into the vacuum chamber. The characteristic of this case is the way in which the amplitude of oscillation builds up as the particle passes repeatedly through the target.

It can again be shown that the loss of a given particle, once it has touched the target, is rather rapid, but the burst can last much longer than in the former case.

Two Target Operation

It is now clear that if two targets are placed in the machine, and the beam is driven outwards, the behaviour of the outside target proceeds as indicated above. The user of the outside target does not notice the presence of the inside one.

When the oscillations have built up sufficiently, the particles touch the inside target which then takes over, and the oscillations die out as before. In this case the inside target user may find some improvement in his beam intensity, since the contacts with his target start at higher energies. He will in any case continue to receive particles for the whole of the burst on the outside target, which may be as long as 80 msecs.

Limitations

It can be shown that multiple scattering modifies the above behaviour only slightly for light element targets (up to, say, carbon) but the system will cease to work for heavy element targets chiefly because of vertical oscillations induced by multiple Coulomb scattering. This should be less serious in the higher energy machines.

It is also necessary that the outside target should be thin, so that the maximum energy loss per target transit should shift the mean orbit only a few millimetres. This makes certain that the inside target receives all the particles which are not absorbed by the outside target no matter what its azimuthal position in the synchrotron may be. The target in use at Birmingham is a vertical polythene wire of 2 mm square section.

An interesting feature of such a thin target, pointed out in the accompanying paper by Booth and Hutchinson[3]), is that it destroys the radio-frequency structure of the beam, which is an advantage in most counter experiments.

The double-target arrangement is in regular use by the counter groups at Birmingham.

[3]) N. E. Booth and G. W. Hutchinson, Nuclear Instruments 1 (1957) 80.

NUCLEAR INSTRUMENTS 1 (1957) 92–93; NORTH-HOLLAND PUBLISHING CO. – AMSTERDAM

MODIFICATION OF THE BROOKHAVEN FAST CHOPPER†

F. G. P. SEIDL††, H. PALEVSKY, D. J. HUGHES, and R. L. ZIMMERMAN

Brookhaven National Laboratory Upton, N. Y.

Received 1 October 1956

The Brookhaven mechanical neutron shutter[1]), or "fast chopper" was designed to produce neutron bursts of 1 μsec length in the energy region from 1 eV to 10 keV. For these energies, hydrogen is the best element for neutron attenuation, and consequently a high strength paper-based phenolic laminate was used to construct the defining slits of the chopper rotor. The attenuation factor of the laminate is approximately 25 per inch over the entire energy interval from 1 eV to 10 keV. Unfortunately, there are two important disadvantages of using hydrogen as the attenuator: 1. the neutron cross section falls at higher energies, therefore the attenuation for unmoderated fission neutrons is weak; 2. hydrogenous materials have a low stopping power for gamma rays, which are plentiful in beams from reactors.

The first point is usually not troublesome because most neutron detectors use $1/V$ absorbing materials and therefore discriminate strongly against the fission neutrons. The weak attenuation of γ-rays, however, is a serious problem because it limits the efficiency that one can obtain with the usual neutron detectors[2]). In order to counteract the listed disadvantages, the Brookhaven fast chopper has been modified in such a way that six inches of steel are in the beam path when the rotor is in a closed position. The modification was made by replacing the inner phenolic sections of the earlier design with steel, fig. 1. The increase in stress on the aluminum forgings due to the greater weight of the inner sections was in part offset by using two high strength steel retaining rings on the steel pieces. In addition, the number of bolts holding the two aluminum forgings together was increased from 16 to 24.

The steel-core rotor was spin-tested and, similar to the former rotors[3]), the phenolic arms at the periphery of the rotor failed at approximately 12 000 rpm. The arms were replaced and the rotor was installed at the Brookhaven reactor. It has been operating in a routine manner on a regular 24 hour schedule for the last six months, during more than half of this time with the rotor spinning at 10 000 rpm. For low neutron energy data the rotor is run at reduced speeds.

Several tests have been made to measure the gamma ray attenuation properties of the new rotor, using a bank of 64 2″ diameter ZnS-B_2O_3 scintillation counters[4]). This neutron detector has a distinct advantage relative to BF_3 proportional counters, because the detection signal is extremely fast (compared to the collection time of ≈ 1 μsec in a typical BF_3 counter) and the flight time in the detector is very short because of its small size in the direction of neutron motion. The counting rate versus discriminator bias setting data were taken with the old, then with the new rotors in closed positions. The ratio of these rates as a function of discriminator setting is shown in the lower curve of fig. 2. At discriminator settings above 20 volts the detec-

† Work performed under contract with U. S. Atomic Energy Commission.

†† Now at Boeing Airplane Company, Seattle, Washington.

[1]) Seidl, Hughes, Palevsky, Levin, Kato and Sjöstrand, Phys. Rev. **95** (1954) 476.

[2]) Palevsky, Muether and Stolovy, Phys. Rev. **93** (1954) 920 (A).

[3]) F. G. P. Seidl, Brookhaven National Laboratory Report 278 (1954) (T-46).

[4]) Palevsky, Zimmerman and Muether, to be published.

Fig. 1. A view of the Brookhaven fast chopper with the upper aluminum forging removed, showing the position of the steel inserts and the lower retaining ring. In the earlier models the entire slit defining system was made of phenolic plastic and the retaining rings were aluminum.

tor is insensitive to γ-rays and the ratio is unity within experimental error, for only fast neutrons penetrating the rotor, plus room background, are being detected. Below 20 volts the ratio rises as γ-rays, more abundant with the old rotor,

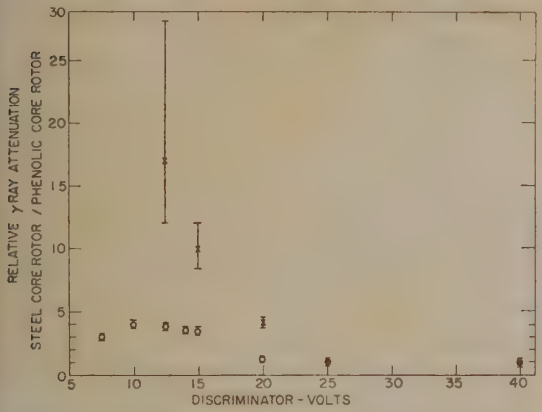

Fig. 2. The open circles are the ratio of counting rates obtained with the steel core and with the phenolic core rotors in a closed position. The crosses are the same taken with tube noise subtracted before taking the ratio of counting rates and represent the relative γ-ray attenuation of the two rotors.

begin to be detected, then reaches a maximum value of four and decreases. The reason for the decrease is that the tube noise becomes a more important contribution than the γ-rays at the low bias settings. In order to clarify the effect of the difference in rotors, the same data are shown in the upper curve of fig. 2, with the tube noise subtracted from both sets of data. The curve now rises monotonically with decreasing bias, and at a discriminator setting of 10 volts the γ-ray counts are seen to be attenuated by a factor of about 20 with the new, relative to the old, rotor. The relative attenuation of 2.5 MeV γ-rays (the mean energy for fission γ-rays) is estimated to be 50 from the theoretical γ-ray cross section, and the attenuation of fission product γ-rays (mean energy 0.7 MeV) should 2 000. The observed counting rate attenuation ratio of 20 at 10 volts bias is a result of the sensitivity of the detector, for this pulse height corresponds to a very high energy gamma ray, above 3 MeV probably.

On the basis of these results the scintillation detector is at present being modified in order to reduce the tube noise, which at present gives a higher counting rate than the γ-rays. It is estimated that the new rotor will make it possible to operate the scintillation detector at a bias setting where the neutron counting rate will be a factor of five higher than with the previous rotor, corresponding to a neutron efficiency of approximately 5 percent at 1 keV. The flight path in the detector is only 0.3 cm and the decay time of the phosphor about 0.1 μsec. Under these operating conditions the detector has reasonable efficiency and is extremely fast relative to a BF_3 counter.

NUCLEAR INSTRUMENTS 1 (1957) 94; NORTH-HOLLAND PUBLISHING CO. – AMSTERDAM

TWO LITHIUM ION SOURCES FOR ACCELERATORS

I. CORNIDES, J. ROÓSZ and A. SIEGLER

Central Research Institute for Physics, Department for Atomic Physics, Budapest

Received 15 August 1956

Two types of Li ion sources developed for the investigation of charge-exchange and nuclear reactions by accelerated Li ions, are described and preliminary results concerning their performance are given.

Early this year investigations of nuclear transmutations induced by accelerated Li ions were planned with attention mainly to Li-Li reactions. First results of these kinds of experiments have recently been reported by Allison *et. al.*[1]).

The accelerators of the Institute being at our disposal the main problem has been to develop a suitable Li ion source. Two types of sources have been tested. On the one hand we have built a modification of the conventional Thonemann source[2]) working in our accelerators as proton source. The discharge vessel received a side extension into which a nickel tube containing lithium was placed. This tube closed at one end and flattened only at the other may be heated electrically from outside. To maintain a steady discharge a support gas proved to be necessary. Magnetic analysis of the ion beam obtained (in the case of H_2 as support gas) showed the following composition:

ion component	Li^+	Na^+	H^+	H_2^+	H_3^+
intensity (μA)	0.5	40	40	15	2

The intense Na^+ component is caused by the Na impurity of the lithium metal used.

The other type we considered useful to experiment with is the thermal source. Surface coatings using different salts of lithium have been prepared long ago as thermal Li^+ emitters for mass spectroscopy and ion microscopy. As the best of these proved to be a lithium aluminium silicate, namely eucryptit[3]). We also started with this subtance produced by melting together lithium carbonate, alumina and silica in a platinum crucible at about 1400 C°. Later, however, to make the melting process easier we altered the composition in the following manner:

	Li_2O	Al_2O_3	SiO_2
eucryptit	11.5%	40.5%	48%
new glass	15.2%	14.8%	70%

This new Li glass exhibited a much lower melting point and working temperature of the emitting layer. In order to prepare this layer the glass was finely powdered and its suspension in amylacetate with some collodium binder painted on to a platinum or molybdenum plate which was heated indirectly. The Li^+ current density obtainable is of the order of 0.1 mA/cm², rather steady and very pure after the rapid decrease of the Na^+ and K^+ components in the first period of heating.

Further investigations are in progress to improve both sources (e.g. to find out the best possible composition of the Li glass) and at the same time experiments have been in order to produce negative and doubly and triply charged positive ions by charge exchange effects.

Thanks are due to Prof. K. Simonyi for many valuable suggestions and his continuous interest regarding this work.

[1]) S. K. Allison *et al.*, Phys. Rev. **102** (1956) 1182.

[2]) S. D. Moak *et al.*, Nucleonics **9** (1951) 3.

[3]) e. g. M. Gauzit, Ann. Phys. (Paris) **9** (1954) 683.

NUCLEAR INSTRUMENTS 1 (1957) 95–100; NORTH-HOLLAND PUBLISHING CO. – AMSTERDAM

ELECTRONIC TIME ANALYZER APPLIED TO THE MEASUREMENT OF THE HALF-LIVES OF METASTABLE NUCLEAR STATES

PER-ARNE TOVE

The Gustaf Werner Institute for Nuclear Chemistry, Uppsala

Received 13 December 1956

An electronic 20 channel time analyzer has been applied to the measurement of the half-lives of metastable nuclear states in the 100 μsec region. The electronic circuits are described and measurements principles discussed, with special regard to the possibility of measuring longer-lived states.

Introduction

The differential delayed coincidence method is commonly used for the measurement of the life-times of excited nuclear states with half-lives ranging from 10^{-10} sec into the μsecond region[1]).

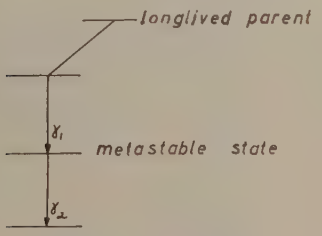

Fig. 1. Decay Scheme

For greater life-times the method becomes less suitable, because of the weak sources and long measurement times which have to be used in order to ensure a sufficient ratio of true to chance coincidences. In this case it is of value, in saving time, to have a system which allows the simultaneous collection of data for different delay times. Consider the simple decay scheme of fig. 1 where the metastable state, with mean life τ, is fed with one γ, γ_1 and in decay gives a second γ, γ_2. Then τ can be measured by an electronic time analyzer consisting of a number of gated count channels which are open for a short time and are successively opened and shut in turn. γ_2 is accepted in these channels, and γ_1 starts the "channel sweep" i.e. the successive opening and shutting of the channels. When the counts in the channels are plotted against channel number a straight line is obtained on a semilog paper. The slope is determined by the mean life of the state.

Description of the Electronic Time Analyzer

Reference is made to figs. 2 and 3. γ-rays from the source are detected in a NaI(Tl) crystal. The pulses are fed in parallel to two amplifiers each with a built in single-channel pulse-height analyzer of the two discriminator-anticoincidence type.

The channel sweep is started by the output of that analyzer which is set to accept the γ_1 rays. The pulse triggers a univibrator whose output gates a ringing LC oscillator circuit with positive feedback[2]). The resulting sine wave train, lasting as long as the univibrator pulse (≈ 10 periods) is shaped in a discriminator-type amplitude comparator to give two separate trains of pulses appearing at the zero passages

[1]) R. E. Bell in Beta and Gamma-ray Spectroscopy, edited by Kai Siegbahn (North Holland Publishing Co., Amsterdam, 1955) p. 506.

[2]) See Electronics, Experimental techniques by W. C. Elmore and M. Sands (McGraw Hill, 1949) for a discussion of this, and other circuit elements.

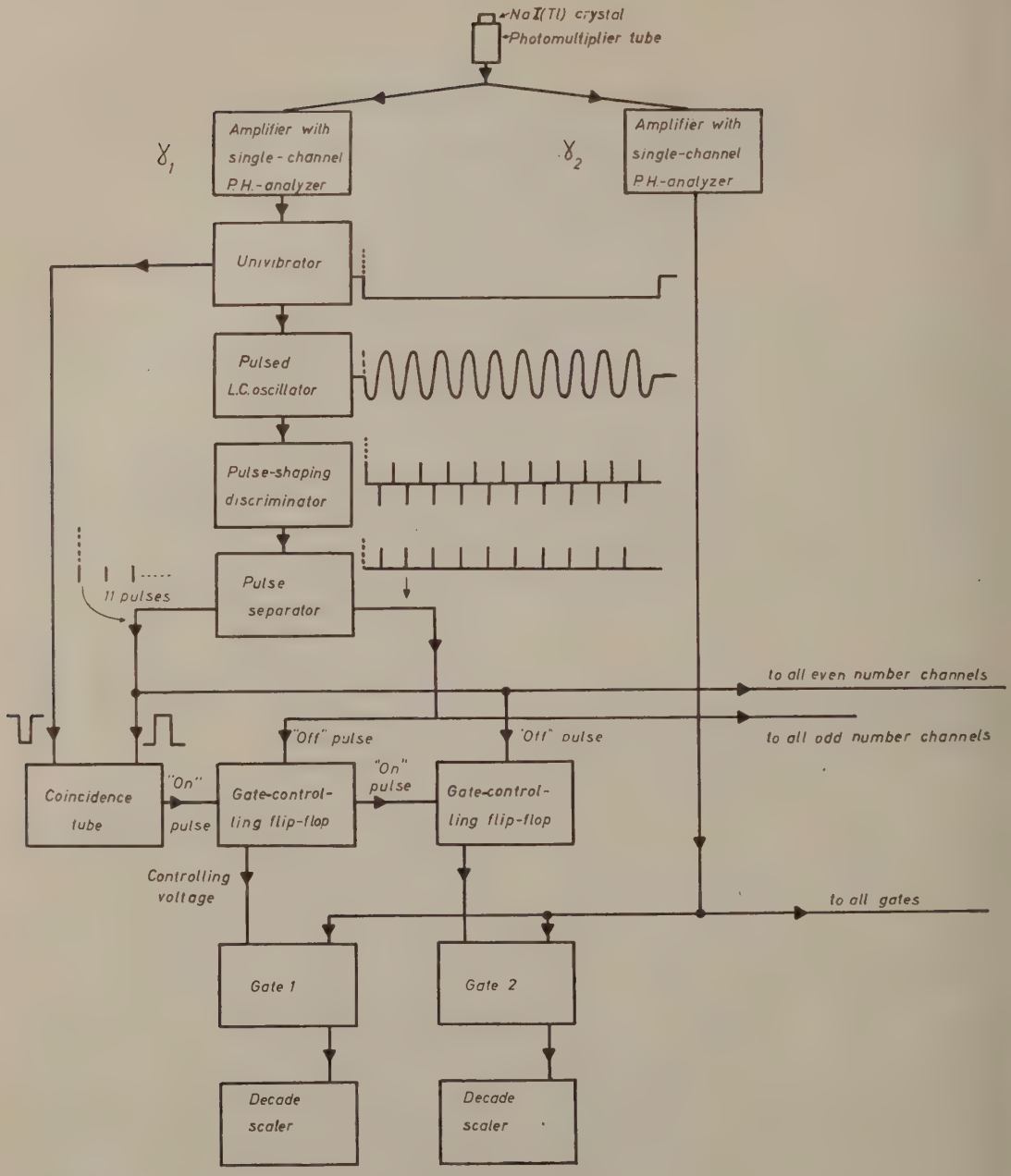

Fig. 2. Schematic Diagram.

Fig. 3. Diagram.

Values for the components are:

$20\,t_k$	100 μs	265 μs	750 μs	2 ms	5 ms
Rl	820 k	820 k	1.5 M	1.5 M	1.5 M
Cl	1000 p	2500 p	2750 p	0.01 μ	0.025 μ
L	2×5 mH	2×10 mH	2×15 mH	2×75 mH	2×110 mH

$20\,t_k$	100 μs	265 μs	750 μs	2 ms	5 ms
C	550 p	1000 p	5000 p	7500 p	0.025 μ
R	27 k	22 k	2.2 k	4.7 k	3.9 k
C2	20 p	20 p	100 p	200 p	500 p

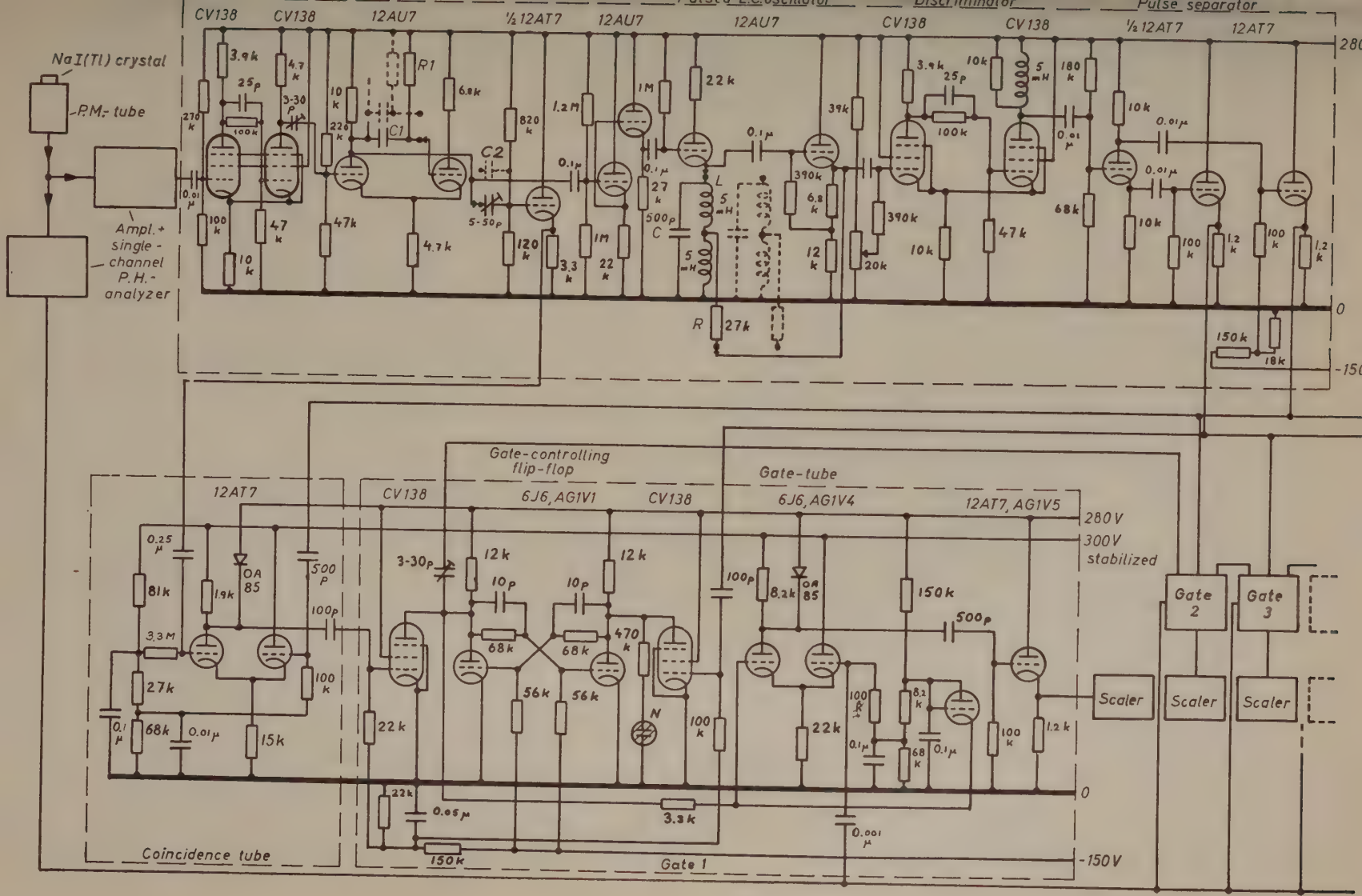
CV138
CV138
12AU7
½12AT7
12AU7
12AU7
CV138
CV138
½12AT7
12AT7
Pulse separator
NaI(Tl) crystal
P.M.-tube
Ampl. + single-channel P.H.-analyzer
R1
C1
C2
R
L
C
280
0
-150
12AT7
CV138
6J6, AG1V1
CV138
6J6, AG1V4
12AT7, AG1V5
Gate-controlling flip-flop
Gate-tube
280 V
300 V stabilized
0
-150 V
Coincidence tube
Gate 1
Gate 2
Gate 3
Scaler
Scaler
Scaler

of the sine wave. The first train consists of pulses, called even pulses, which appear when the sine wave is zero and becoming negative. The other train, consisting of "odd pulses", appears when the sine wave becomes positive. In some experiments a different pulse shaper, based on a window amplifier, was used.

The pulses are shortened by a pulse-shaping inductance in the anode of the discriminator and control the opening and shutting of the gates of the 20 channels in turn. Each channel consists of a d.c.-controlled gate and a decade scaler. When a gate is open, γ_2 pulses, which are fed to all gates in parallel, can pass to the corresponding scaler.

The first of the "even" control pulses comes at the same time as the front edge of the univibrator pulse. These two pulses are taken in coincidence to open the first gate. It is shut a half sine-wave later by the odd pulses, which are connected to shut all open odd-number gates. When the first gate is shut, it gives an opening pulse to the second gate. This is shut a half sine-wave later by the even pulses, which are connected to shut all open even-number gates. In this way the "channel sweep" proceeds through all gates of the 20 channels.

The coincidence opening of the first channel ensures that this is open for the same length of time as the others. The switching of the discriminator is not done exactly at the zero passages of the sine-wave but the timing error is easily seen to be very small when the sine-wave is 20–30 V. In addition, the d.c. bias of the discriminator is set so that the error caused by the discriminator bias balances out the error introduced by the inherent small discriminator hysteresis, in effect giving equal open times for even and odd gates. The equality and the open time of the channels are checked by an oscilloscope or more exactly by feeding unrelated pulses at known rates to the "channel sweep" input and the channel inputs. An input discriminator ensures uniform, not too hard, triggering of the univibrator. A cathode-follower is inserted between univibrator and L.C.-oscillator to prevent retriggering at the end of the period.

Each channel gate consists of a flip-flop tube AG1V1 which controls gate tube AG1V4. In the "open" state of the flip-flop, incoming pulses, which are fed to AG1V4b, shut off the current in AG1V4a and a positive 20 V pulse is fed via cathode-follower AG1V5b to the channel scaler. No output pulse is produced when AG1V1 switches over, as AG1V4 conducts enough current, even when AG1V1a plate is down, to prevent the plate of AG1V4a from rising above 280 V. AG1V5a functions as a grid catching diode if the switching action should take the plate of AG1V1a too far down. Resistor R1 helps in this function as well as in preventing cutting-off of Ag1V4a if the plate waveform of AG1V1 is too fast.

Provision has also been made for increasing the open time of the late channels 2, 4 or 8 times compared with the first channels. This is done by three flip flops constituting a scale-of-eight circuit, which scales down one of the gate-controlling pulse trains. The scaled-down pulses which are taken from all six anodes of the three flip-flops are used as shut-off pulses for the later channels instead of the even or odd pulses. It is easily seen that by proper choice of the shut-off pulses for the different gates various ways of operation can be obtained, e.g. first five channels open time t_k, channels 6–10 open $2t_k$, 11–15 open $4t_k$, and 16–20 open $8t_k$. The three flip flops are electronically reset to any desired configuration at the end of the pulse train which for this mode of operation must last longer than the 10 sine wave periods previously mentioned.

The apparatus is part of a combined time-analyzer and pulse height analyzer system, used in various experiments.

Principles of Measurement

Assume a decay of the type indicated in fig. 1. γ_1 is accepted in the pulse-height analyzer which triggers the channel sweep of the time analyzer. γ_1 is detected, i.e. triggers the time analyzer, with an overall efficiency of F_1, including source geometry, detection efficiency, and dead time effects of the time analyzer. Of

the number N_1 counts/sec in the one-channel analyzer the fraction α_1 is actually due to a γ_1 so $\alpha_1 N_1 = F_1 \cdot N$; similarly $\alpha_2 N_2 = F_2 \cdot N$ for the second one channel analyzer, set to accept γ_2. The values of the α:s can be estimated from the shapes of the γ spectra.

Choosing a certain γ_1 at time 0, the probability that its accompanying γ_2 will appear in the interval t_k between times t and $t + t_k$ is

$$\int_t^{t+t_k} \frac{e^{-\frac{t}{\tau}}}{\tau} dt = e^{-\frac{t}{\tau}} \cdot (1 - e^{-\frac{t_k}{\tau}})$$

Here τ is the mean life of the state, giving a probability distribution

$$s(t) = \frac{e^{-\frac{t}{\tau}}}{\tau}$$

for decay.

The fraction of the $\alpha_1 N_1$ triggerings of the time analyzer which gives a true pulse in the time channel at time t is thus

$$e^{-\frac{t}{\tau}} \cdot (1 - e^{-\frac{t_k}{\tau}}) \cdot F_2$$

The true pulses in that channel are thus

$$N_r = F_1 \cdot N \cdot F_2 \cdot e^{-\frac{t}{\tau}} \cdot (1 - e^{-\frac{t_k}{\tau}})$$

per sec.

The time channel sweep is started N_1 times/sec, the open time being t_k for each channel.

Assume $\tau N \ll 1$, neglecting the contribution from γ_2 pulses detected during a later channel sweep than that triggered by their corresponding γ_1. Then, considering all N_2 pulses whose corresponding γ_1 were not accepted, i.e. $N_2 - F_1 F_2 N$, as unrelated to the opening $\alpha_1 \cdot N_1$ pulses; and all N_2 pulses as unrelated to the $(1 - \alpha_1)N_1$ opening pulses, the chance pulses per channel are $N_c = t_k \cdot \alpha_1 N_1 (N_2 - F_1 F_2 N) + t_k (1 - \alpha_1) N_1 \cdot N_2 = N_1 N_2 t_k (1 - \alpha_1 \alpha_2 F_1)$ per second.

Hence

$$\frac{N_r}{N_c} = \frac{\alpha_1 \alpha_2 e^{-\frac{t}{\tau}} \cdot (1 - e^{-\frac{t_k}{\tau}})}{N t_k \cdot (1 - \alpha_1 \alpha_2 F_1)}$$

$$\approx \frac{\alpha_1 \alpha_2 e^{-\frac{t}{\tau}} \cdot \left[1 - \frac{1}{2}\frac{t_k}{\tau} + \frac{1}{6}\left(\frac{t_k}{\tau}\right)^2 + \ldots\right]}{N\tau(1 - \alpha_1 \alpha_2 F_1)}$$

$$\approx \frac{\alpha_1 \alpha_2 e^{-\frac{t}{\tau}}}{N\tau(1 - \alpha_1 \alpha_2 F_1)} \quad (t_k \ll \tau) \qquad (1)$$

For small detection efficiencies, as long as "source background" is most important, the ratio N_r/N_c is not influenced by source geometry and detector efficiencies, but these factors determine the measurement time required for a given number of counts. For weaker sources and longer life-times "general background" becomes important. Then it is favourable if the source detection efficiency can be increased, without proportionately increasing the general background count rate. This points towards using a hollow γ-crystal.

It is reasonable that when $\alpha_1 = \alpha_2 = F_1 = 1$ no false pulses are obtained as the channel sweep is never started at a wrong time ($\alpha_1 = 1$) and no γ_2 pulses not belonging to the decay are accepted ($\alpha_2 = 1$). $F_1 = 1$ ensures that two true γ_2 pulses belonging to different decays cannot be accepted during the same channel sweep.

If the chance pulses in each channel can be calculated from N_1 and N_2, t_k and the measurement time T_m, the total open time of the analyzer should not be more than one or two half-lives in order to secure a high N_r/N_c ratio for the later channels.

When the metastable state is fed from a nucleus with a rather short half-life, it is of interest to make the measurement time as small as possible. To give an idea of the time needed, take as a conservative example F_1 and $F_2 = 0.02$, which could be obtained[3]) at 300 kV with the source close to a 1″ NaI crystal. Assume $\alpha_1 = \alpha_2 = \frac{1}{2}$, and allow $N_r/N_c = 2$ in the first channel. Then to obtain 1000 pulses in this channel, the measurement time, T_m, is $1000/N_r$, and from (1)

$$\frac{N_r}{N_c} = \frac{\frac{1}{4}}{N\tau(1 - 0.02 \cdot \frac{1}{2})} = 2 \text{ gives} N\tau \approx \tfrac{1}{8};$$

[3]) Compare B. Kahn and W. S. Lyon, Nucleonics **11** (1953) 61.

$$N_r = F_1F_2 \cdot N = F_1 \cdot F_2 \frac{1}{8\tau}$$

$$T_m = \frac{1000 \cdot 8\tau}{F_1F_2} = 2 \cdot 10^7 \cdot \tau,$$

giving 68 minutes for a 200 μsec mean life and 56 hours for a 0.01 sec mean life. At longer times the general background comes in, in effect making α_1 and α_2 smaller.

For higher energies the efficiency becomes smaller. Higher efficiencies, and thus smaller T_m, could be obtained by using a hollow γ-crystal.

To estimate roughly the longest life-times that could be measured under very favourable conditions assume that half of the count rate is due to "general background", i.e. $\alpha_1 = \frac{1}{2}$ and $\alpha_2 = \frac{1}{2}$, and $F_1 \approx 1$, which could be approached in a hollow γ-crystal for a certain range of γ-energy. Assume further that $N_r/N_c = 1$ is desired in the first channel. This gives $N\tau = \frac{1}{8}$. Considering $F_1 \approx 1$ and N equal to the general background rate this means that life times not much smaller, perhaps 10 times, than the mean spacing between general background pulses could be measured. For a 2″ diameter hollow crystal shielded with 5 cm lead the background count rate was 0.3 p/sec at 200 kV and 20 kV channel width.

Measurement Example

The measurement of the half-life of the previously reported metastable state[4]) in Pb^{206} will be briefly described here. Referring to the energy level diagram given by Alburger it is seen that the state is fed almost entirely by a 0.184 MeV γ. Using a source containing 6 day Bi^{206}, the γ_1 channel was set to accept this line. The metastable state decays almost entirely by a 0.516 MeV E3 transition. The γ_2 channel was adjusted to this energy. With the hole crystal, two weak sources of relative intensities 1.7 and 0.35 were used, giving respectively 3.2 and 17.4 for the ratio N_r/N_c in the first channel and respectively 3.5 and 0.9 true counts per min. in this channel. The 1″ crystal and the strongest source gave 3.4 for N_r/N_c and 0.7 true pulses per min. in the first channel. These figures agree substantially with the predictions of eq. 1. When put into the equations they indicate somewhat smaller values for α and F than those used in the discussion of T_m. The value obtained for the half-life of the state was 123 ± 4 μsec. The chance pulses were calculated from $N_c = N_1 \cdot N_2 \cdot t_k$, and $t_k = 14.7$ μsec was used.

It was found that a higher N_r count rate and a good N_r/N_c-ratio could be obtained by accepting all γ energies in both channels. This can be explained by higher detection efficiency following from the existence of many γ:s in cascade with, and preceeding, the 0.184 MeV transition, and several γ:s in cascade with, and succeeding, the 0.516 MeV transition, and the absence of strong crossover lines.

Acknowledgements

The author wishes to thank Prof. The Svedberg for support of this work. He also thanks Prof. K. Siegbahn for his encouraging interest. A stimulating contact was held with Dr. I. Bergström. Mr. P. Isacsson and Mr. S. Sundell helped with the electronics.

The work has been supported by the Swedish Atomic Energy Commission.

[4]) D. E. Alburger in Beta and Gamma-ray Spectroscopy, loc. cit. p. 707.

NUCLEAR INSTRUMENTS 1 (1957) 101–106; NORTH-HOLLAND PUBLISHING CO. – AMSTERDAM

PRECISION QUANTAMETER FOR HIGH ENERGY X-RAYS†

ROBERT R. WILSON

Cornell University, Ithaca, N.Y.

Received 2 January 1957

An ionization chamber has been designed to serve as a standard for measurements of the intensity of beams of high energy photons. The chamber consists of twelve plates of copper, each of one cm thickness, so that nearly all the energy of the photons is absorbed in the chamber. The ionization in the shower is sampled at the twelve gaps between plates, and the gap widths are arranged so that a Simpson's rule integration of the shower curve is automatically made. By making the last gap larger and by making an appropriate gap at the sides of the chamber, a compensation is made for any leakage of energy out of the chamber.

The total energy content of a photon beam, U, should be accurately proportional to the ionization charge measured, q, independently of the spectral shape of the beam. An absolute calibration of the chamber has been calculated to an accuracy of a few percent. A density effect correction to the stopping power of copper has been included in the calculation.

Before an electron synchrotron or betatron can be used for quantitative experiments, the energy and intensity of the photon beam must be calibrated. Pair spectrometer measurements[1]) have indicated that the energy distribution of the X-rays is precisely the bremsstrahlung spectrum predicted by theory[2]). The overall intensity of the photon beam can then be characterized by its total energy content U or by Q, the number of equivalent quanta. These are defined and related in the following manner:

$$U = \int_0^{E_0} n(k)\, k\, \mathrm{d}k \qquad (1)$$

and

$$Q = U/E_0 \qquad (2)$$

where k is the photon energy and E_0 is the energy of the electrons producing the X-rays.

Perhaps the most direct measurement of U is by the calorimetric device of Kerst[3]). One can also determine U by making a shower curve using absorbers and a thin ionization chamber after the method of Blocker, Kenney and Panofsky[4]), and it is this method that is the basis of the ionization chamber or "Quantameter" to be described here.

In the shower method it is assumed that all of the energy of the incident photons eventually is lost to ionization and excitation of the stopping medium. Since only the ionization is measured, it is also assumed that the energy loss per ion pair formed is independent of the electron energy. Furthermore, since the ionization is measured in the gas of the ion chamber whereas one wishes to know the energy loss in the dense stopping material, the relative stopping powers of gas and solid must be known.

Normally in applying the shower method, one measures the ionization at various depths of absorber, plots out a shower curve, integrates it, and then computes U or Q for the beam. A more convenient ionization chamber is then calibrated and used as a secondary standard. The difficulty with this procedure is that the calibration constant of the secondary standard usually depends on the energy of the incident photons.

The ionization chamber shown in fig. 1 has been designed to combine both functions. It automatically makes an integration of the shower

†) Supported by the joint program of the Office of Naval Research and the U.S. Atomic Energy Commission.

[1]) J. DeWire and L. Beach, Phys. Rev. **83** (1951) 476; J. Lawson, Phys. Rev. **75** (1949) 433.

[2]) H. A. Bethe and W. Heitler, Proc. Roy. Soc. **146** (1936) 84.

[3]) P. D. Edwards and D. W. Kerst, Rev. Sci. Instr. **24** (1953) 490.

[4]) W. Blocker, R. Kenney and W. Panofsky, Phys. Rev. **79** (1950) 419.

curve, hence its calibration should be independent of the energy or spectral shape of the incident photons. In addition, it should be possible to compute the absolute value of the calibration constant. The design has been made so that standard materials are used and so that it should be possible to duplicate it in an ordinary machine shop.

face of the outer cover together with the end-support plate constitute the equivalent of the first one cm thick plate. A precision pressure meter is placed at the rear to monitor pressure. A mixture of 95 % argon plus 5 % CO_2 is used to fill the chamber to a total pressure of 800 mm Hg measured at 20° C. The charge, q, collected in the chamber is measured by the vacuum tube

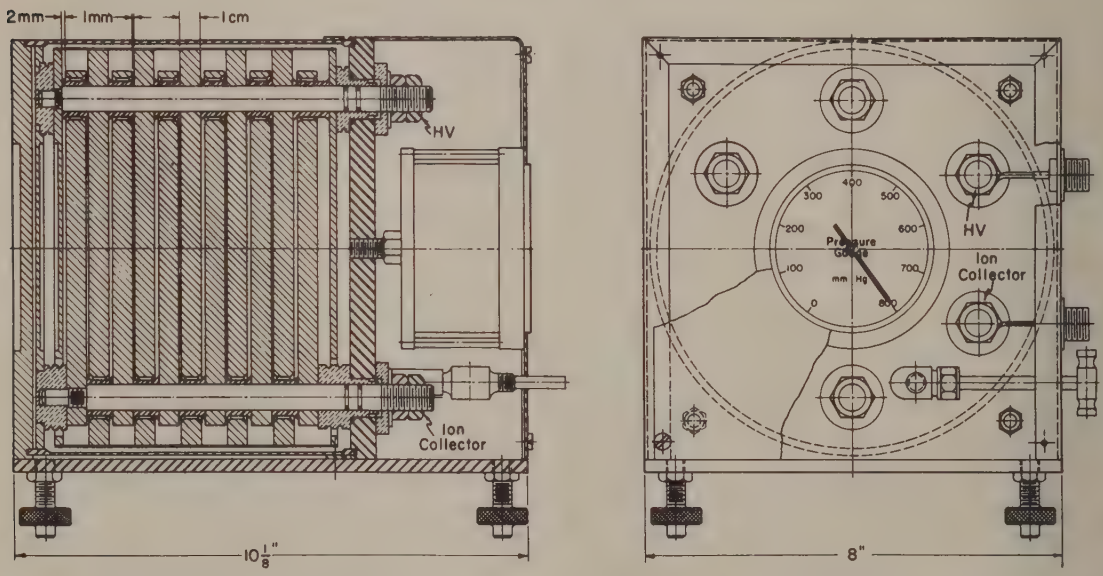

Fig. 1. On the left is a cross sectional view along the axis of the quantameter. The X-ray beam enters from the left. The view at the right is of the back of the quantameter.

The chamber consists essentially of twelve electrolytically pure copper plates which are accurately machined to a thickness of one cm and which are spaced alternately 2.00 and 1.00 mm apart, except for the last gap which is made 6.5 mm. The plates are connected together in such a manner that high voltage appears on half the plates, the other half receiving the ionization current. The two sets of plates are supported independently by three stainless steel rods for each set, and accurate spacing is determined by stainless steel sleeves on these rods. After assembly of the plates on the base plate, the spacing can be checked before the outer covers are put in place. It was found possible to hold the spacings to an accuracy of one mil ($\pm$ 0.0025 cm) in our shop. The front

electrometer and integrator designed by Littauer[5]).

The total energy U in the beam is given by

$$U = r\, w\, q/e \tag{3}$$

where w is the energy loss per ion pair formed in the gas, r is the ratio of energy loss in the copper to energy loss in the gas and e is the charge of an electron. We must first ask how well the total energy loss in the copper is measured by the rather widely spaced samples of ionization. What we are trying to do is to integrate a shower curve in the copper, and this is done by a built-in application of Simpson's rule, i.e.

$$I = \tfrac{1}{3} x_0 [i_0 + i_{12} + 4(i_1 + i_3 + \ldots + i_{11}) + 2(i_2 + i_4 + \ldots + i_{10})] \tag{4}$$

[5]) R. M. Littauer, Rev. Sci. Instr. **25** (1954) 148.

where x_0 is the interval of thickness and i_n is the ionization density at the n^{th} gap. Now i_0 is assumed to be zero for photons and hence is not measured. The above sum is made automatically by making the odd gaps 2 mm wide, the even gaps one mm.

The last gap would be made one-half mm wide except for the following consideration: Although the ionization at the last gap has fallen to a small fraction of its value at the peak, we would miss a few percent of the area of the shower curve by not continuing the chamber to greater thicknesses. We know, however, that the tail of the shower falls exponentially with a decay constant characterized by the minimum value of the absorption coefficient of copper for gamma rays. The measurements of Blocker *et al.*[4]) give 4.0 cm for this mean free path. Thus we can increase the thickness of the last gap so that we automatically measure and then add the ionization current which would obtain in all the additional gaps occurring in an infinitely deep chamber. This gap width turns out to be 4.0 times the average gap width of the rest of the chamber which is 1.5 mm, hence the 12^{th} gap is made 6.0 mm + 0.5 mm wide.

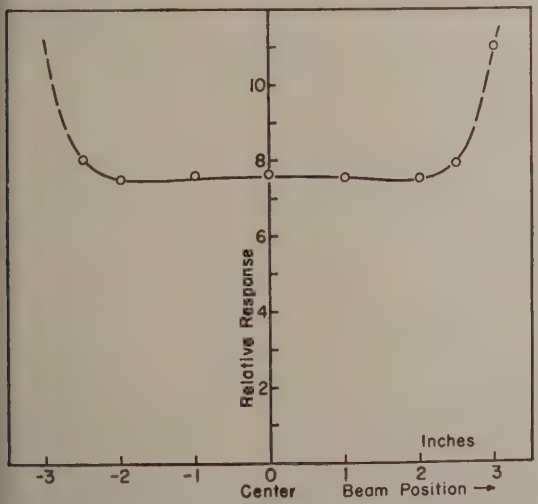

Fig. 2. The relative response of the chamber to a narrow pencil of 800 MeV X-rays about one cm in diameter and parallel to the axis of the chamber, is plotted as a function of the distance from the axis. The increase at the edge is due to the beam passing directly through the compensation gaps at the edges of the plates.

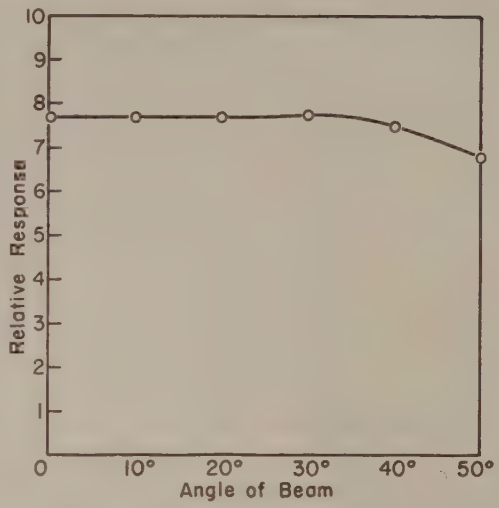

Fig. 3. The relative response of the chamber to a narrow pencil of 800 MeV X-rays which enter the chamber in the center at the front but at an angle with respect to the axis of the chamber that is indicated on the graph. At 45°, the beam passes through only six plates, illustrating the effectiveness of the compensating gaps at the sides of the chamber.

The same procedure can be used to correct for lateral leakage. Any gamma radiation propagating at right angles to the initial beam direction must necessarily be of very low energy and should be characterized again by the minimum in the transmission of the copper. It can be seen in fig. 1 that the region between the outside edges of the collector plates and the cylinder which encloses the high voltage plates constitutes an additional ionization chamber and the radii of the two sets of plates have been chosen so that the volume is equivalent to that of a continuous gap of 6 mm width enclosing the chamber. This makes the additional ionization collected there just compensate for that part of the shower which leaks out of the chamber laterally. Originally a chamber was constructed to have twenty plates. The compensation worked so well that the number of plates was then reduced to twelve.

The effectiveness of the compensation is illustrated in figs. 2 and 3 where the response of the chamber for a given number of "Q" is plotted under varying conditions of incidence of

a narrow, about one-half inch thick, beam. In fig. 2, the beam is kept parallel to the axis but its radial position is varied. In fig. 3, the beam enters the chamber on the axis but at varying angles with respect to the axis. The constancy if the energy loss per ion pair should turn out to be dependent on electron energy because the distribution of electron energy in a developed shower is essentially independent of the incident photon energy. The range of proportionality

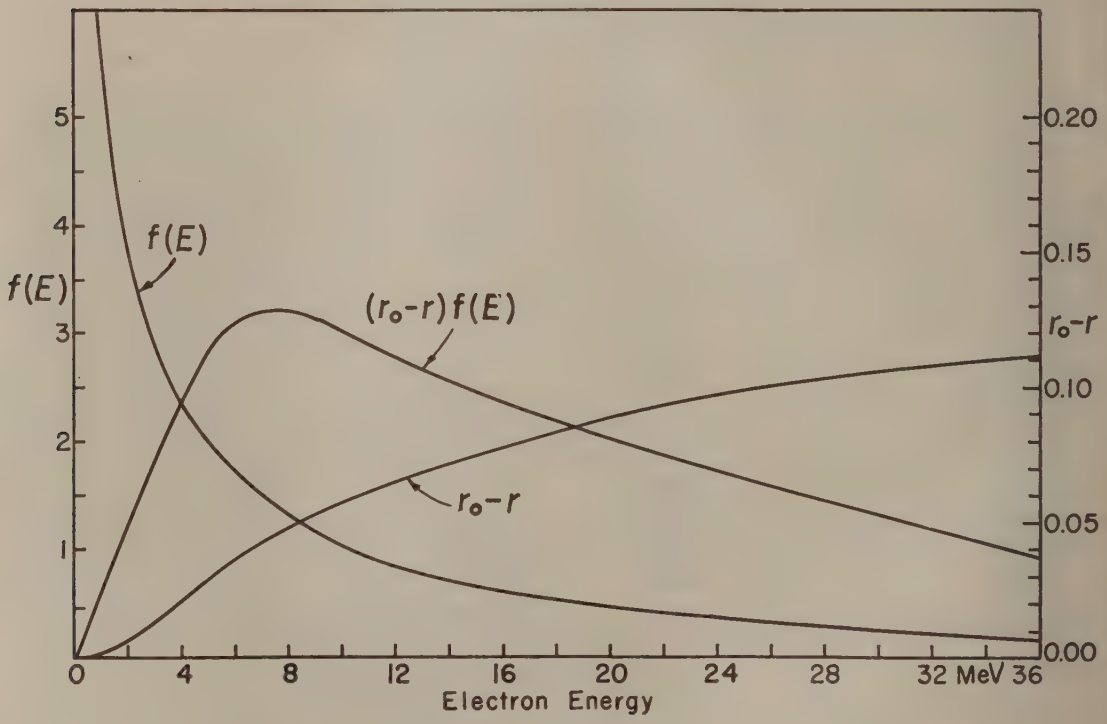

Fig. 4. The track length is 0.437 E_0 $f(E)$, where E_0 is the initial X-ray energy and $f(E)$ is plotted above as a function of the electron energy in the shower. The quantity r measures the variation with electron energy of the stopping power, dE/dx, of copper relative to the gas. The value of r_0 is 0.942 and refers to r at very low energy. The curve marked $(r_0 - r) \times f(E)$ is the product of the other two curves and was integrated numerically to obtain an average value of r for the shower electrons

of these curves over so wide an interval of the variants is a gratifying demonstration of the effectiveness of the compensation.

From the above we see that the energy in the beam U should be accurately proportional to the charge q produced by the ionization. If we can calibrate the constant of proportionality at one energy, say at 300 MeV, by using a pair spectrometer, then the same constant should be valid at any other energy. This will be true even should extend from a few MeV to well above 100 GeV.

The quantameter has been compared at 300 MeV to the Cornell thick ionization chamber which in turn was calibrated against a pair spectrometer. This gives a value of 4.55×10^{18} coulombs/MeV for the constant q relating U and z.

It is interesting to see how accurately this constant of proportionality can be calculated. With references to equation (3), q is measured and we can

look up w, but r, the ratio of the energy loss in the copper to energy loss in the gas, must be computed as a function of the energy of the electrons in the shower and then an appropriate average must be taken. The appropriate energy distribution of the electrons in the shower is given by the differential track length $f(E)$, i.e. the distance travelled by electrons with energy between E and $E + \mathrm{d}E$. This has been computed rather accurately by Richards and Nordheim[6]). They find little difference between air and lead, showing that the Z dependence is negligible, if the answer is put in units of the critical energy and radiation length which are 21.5 MeV and 12.8 g/cm² respectively for Cu. Fig. 4 shows a curve of $f(E)$ as a function of electron energy for Cu. About half the integral of $f(E)$ is below or above 10 MeV, and 90 % of the total track length lies below 80 MeV or above one MeV, which gives us an idea of the important range of electron energies in the shower.

Sternheimer[7]) gives the following formula for the energy loss in MeV per gram per cm³ of electrons:

$$\frac{\mathrm{d}E}{\mathrm{d}x} = A\,[B - 1.4 + 3\ln(p/mc) - \delta] \qquad (5)$$

where p/mc is the momentum of the electron and A, B and δ are constants depending on the material the most recent values of which are also given by Sternheimer[8]). The constant δ corrects for the density effect and is very important for electrons. The ratio, r, of energy loss in Cu to that in gas was computed for different values of energy using equation (5). The results are plotted in fig. 1 which also shows the track length distribution. In order to obtain the average value of r over the track length, the two curves of fig. 4 were multiplied together and the result was numerically integrated from zero to 32 MeV, the rest of the integral being computed from the integral track length value for all electrons above 32 MeV which is also given by Nordheim and Russel. The resulting average value of r for pure argon is 0.883 $(\rho t)_{\mathrm{Cu}}/(\rho t)_{\mathrm{argon}}$, and for the mixture of 760 mm Hg of argon and 40 mm Hg of CO_2 this value of r must be corrected by one percent which makes it become $0.873(\rho t)_{\mathrm{Cu}}/(\rho t)_{\mathrm{gas}}$.

The relation between charge measured and total energy can now be written

$$U = 0.873\ (wq/e)\ (\rho t)_{\mathrm{Cu}}/(\rho t)_{\mathrm{gas}} \qquad (6)$$

The density of the copper used was obtained by weighing and measuring the copper plates and it was found to have the value 8.91 g/cm³. The plates were also found to be uniform in thickness and density from one plate to another to an accuracy of 0.2 %. The density of argon at 0° C. and 760 mm Hg is given in handbooks as 1.784 mg/cm³ and that of CO_2 for the same conditions is given as 1.977 mg/cm³. The average thickness of the copper plates was 1.000 ± 0.002 cm while the average gap thickness was found to be 0.149 ± 0.002 cm.

Curran, Angus and Cockcroft[9]) as well as Weiss and Bernstein[10]) have measured 25.5 ± 0.3 eV per ion pair for the value of w for electrons in argon which agrees with the value measured by Bakker and Segre[11]) for 340 MeV protons in argon. Nicodemus[12]) found 26.9 eV per ion pair for 17.4 keV electrons which indicates just how insensitive w is to the energy of the electrons. Let us adopt 25.5 eV per ion pair for w until a better measurement is indicated. Weiss and Bernstein also give 32.6 ± 0.4 eV per ion pair for the value of w for CO_2 which makes the average value of w for our CO_2-A mixture be 26.9 ± 0.3 eV per ion pair. Using the above values we get[13])

$$U_{\mathrm{MeV}} = 4.82 \times 10^{18}\ q_{\mathrm{coulombs}} \qquad (7)$$

for the mixture of 760 mm Hg argon and 40 mm

[6]) J. A. Richards and L. W. Nordheim, Phys. Rev. **74** (1948) 1106.

[7]) R. M. Sternheimer, Phys. Rev. **88** (1952) 851.

[8]) R. M. Sternheimer, Phys. Rev. **103** (1956) 511.

[9]) S. C. Curran, J. Angus and A. L. Cockcroft, Phil. Mag. **40** (1949) 36.

[10]) J. Weiss and W. Bernstein, Phys. Rev. **98** (1955) 1828.

[11]) C. Bakker and E. Segre, Phys. Rev. **81** (1951) 489.

[12]) E. Segre, Experimental Nuclear Physics (John Wiley and Sons, Inc., New York, 1953) p. 3.

[13]) For pure 800 mm of Argon the constant would also be 4.82×10^{18} MeV/coulomb.

of CO_2 at 20° C. This calculated calibration constant should be accurate to a few percent which is much better than anything claimed for the present experimental calibrations.

Effects due to ionic recombination can be expected at very high beam intensities, i.e. greater than 10^{12} "Q" per minute. From recombination theory, the charge that is actually measured, q, is related to the charge, q_0, produced in the gas by the very crude expression

$$q/q_0 = e^{-a(U'/VA)} \quad (8)$$

where U' measures the beam intensity in MeV/sec, A is the area of the beam, V is the voltage between the plates of the chamber, and a is a constant to be evaluated experimentally when such large intensities are available. J. W. Boag[14]) has given a rather complete treatment of recombination effects and one may be able to make a quantitative estimate of the loss by reference to that work.

The collection voltage, V, must not be raised to too high a value in order to overcome recombination, because multiplication due to electron collisions in the gas will then occur. With pure argon in the chamber, a one percent multiplication occurs with 200 volts between the plates. It was for this reason that the CO_2 was added, because it was felt that this would keep the electron energy, and hence the multiplication, down. The addition of CO_2 should also decrease recombination effects inasmuch as the drift velocity is thereby increased and thus the electrons will be swept out of the gas more rapidly.

[14]) J. W. Boag, Brit. j. Radiobiology **25** (1950) 649; Boag and Wilson, B.J.A.P. **3** (1952) 222.

NUCLEAR INSTRUMENTS 1 (1957) 107–111; NORTH-HOLLAND PUBLISHING CO. – AMSTERDAM

MULTI COINCIDENCE GONIOMETER FOR ANGULAR CORRELATION MEASUREMENTS

TOR RAGNAR GERHOLM, TORSTEN LINDQVIST

Institute of Physics, University of Uppsala, Sweden

and

HENDRIK DE WAARD

Natuurkundig Laboratorium, University of Groningen, Netherlands

Received 20 October 1956

Four scintillation detectors view the same source. All six coincidence combinations between these are recorded simultaneously. A "coincidence cross delay" speeds up the measurement of angular correlations by another factor of two. It is shown that the instrument is self-monitoring and that the coincidence counting effiency is an order of magnitude higher than in a conventional arrangement with two detectors. It is concluded that the instrument is suitable for the study of very short lived isotopes. The apparatus was checked with the Co^{60} 1.17–1.33 MeV cascade and the Bi^{207} 1.06–0.57 MeV cascade.

1. Introduction

The relative angular distribution between successive nuclear gamma-rays or conversion electrons depends on the multipolarities of the corresponding transitions. Angular correlation measurements, therefore, provide a useful tool for determining spins and parities of nuclear levels[1]). As is well known, the general procedure is to use two detectors viewing the same source. One detector is kept fixed while the other is rotated around the source. The number of coincidences is recorded as a function of the angle between the two detectors. Corrections should be applied for the finite solid angles of the two counters and for the decay of the radioactive source. To reduce systematical errors caused by instability in the electronics it is preferable to change the angle between the two counters frequently and to repeat the measurements for each angle many times. For this reason angular correlation instruments are generally automatized.

The method suffers from certain limitations. Of course, only levels de-excited by cascade-transitions can be used. The measurements do not always give a unique answer and complimentary experiments may have to be carried out, e.g. measurements of internal conversion coefficients.

Since it is necessary to get a very good statistical accuracy one has to run the experiment for quite a long time. This implies that one is restricted to reasonably long-lived isotopes.

With the *Multi Coincidence Goniometer* (MCG) described in this paper, especially this last limitation is to some extent overcome. The basic idea is to use several detectors and to record the coincidences between any two of these detectors simultaneously. In our present MCG four detectors are used, suitably distributed on a circle around the source.

2. The Block Diagram

Each detector consists of a NaI (Tl) crystal fixed to a photomultiplier tube followed by a cathode follower and a linear preamplifier (cf. block diagram fig. 1: Counter + Preampl).

From the linear amplifier in each channel the pulse spectrum is fed into a limiting amplifier (Limiters) giving a positive output pulse of about 7 volts height for any input pulse greater than 0.4 volts.

[1]) H. Frauenfelder, Beta and Gamma Ray Spectroscopy, Editor Kai Siegbahn (1955) Ch XIX (I).

The output pulses go to a fast coincidence unit (Fast coinc.) which has an adjustable resolving time normally set at 0.1 μsec.

When pulses from any two counters are in coincidence the fast coincidence unit delivers a negative output pulse to a "conditioned gate" (Gates) in each channel. Actually these gates are built in the same unit as the limiting amplifiers. The unit delivers output pulses to two rows, each of six terminals.

The first row is connected to the final gate (Final Gate). Each pair combination of the detectors corresponds to a terminal of this row.

The second row is connected to the main gate (Main Gate), where it delivers pulses (routing pulses) to *two* terminals for each pair combina-

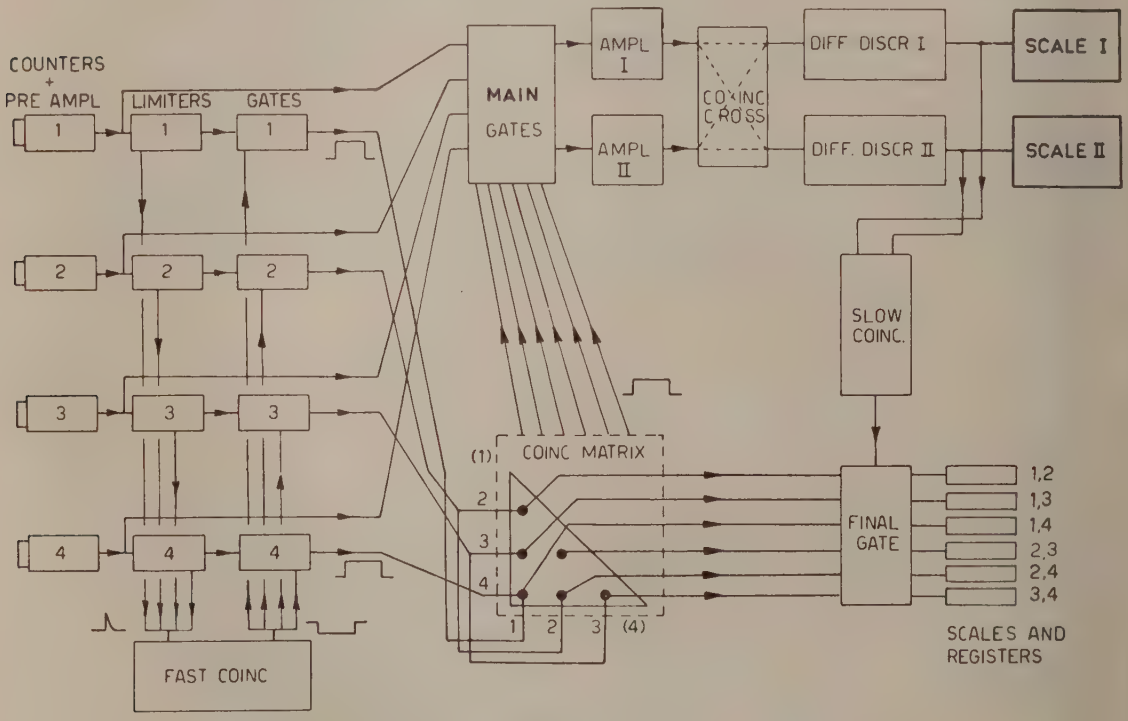

Fig. 1

Each of these gates acts as follows: a positive output pulse is produced from it only if the input pulse from the fast coincidence unit coincides with a pulse from the corresponding limiting amplifier. Thus pulses of exactly the same width and starting at exactly the same moment occur at the outputs of any two channels between which a coincidence has occurred.

From the conditioned gates the pulses go to a "coincidence matrix" (Coinc. Matrix), which determines between which two counters the coincidence has occurred. The principle of the coincidence matrix can be seen in the diagram. tion. The routing pulses from the coincidence matrix rout the output pulse from the linear preamplifiers in such a way, that always one of two coincident pulses occurs at output I of this gate and the other at output II. The output pulses from the main gate are similar in appearance to the input pulses. These pulses can therefore be used for energy selection.

This energy selection takes place in the conventional way by means of differential discriminators preceded by two linear amplifiers. The output pulses from the discriminators are fed to a slow coincidence unit (Slow Coinc.). This part

of the MCG operates in principle as an ordinary two-channel coincidence spectrometer. However, as shown in the block-diagram we have introduced here a "coincidence cross delay" (Coinc. Cross), which improves the coincidence counting efficiency by a factor of about two. It works in the following way. A coincident pair of pulses will be presented "directly" (amplifier I to discriminator I, amplifier II to discriminator II) as well as "crossed" (amplifier I to discriminator II, amplifier II to discriminator I) in the latter case with a delay of 3 μsec. Of course the "crossed" coincidences will give identically the same angular correlation as the "ordinary" coincidences. By means of the coincidence cross delay the useful coincidence counting rate is effectively doubled. Such a coincidence cross may be introduced to good advantage in any two channel coincidence spectrometer with identical detectors. From the output of the slow coincidence unit signals are fed to the final gate.

The final gate transmits the pulses from the coincidence matrix (first row) to the register units, provided there comes a pulse from the slow coincidence unit. Thus we obtain for each detector combination the number of coincidences that have fulfilled the energy conditions set by the differential discriminators. These coincidences are recorded on six register units representing the combinations 12, 13, 14, 23, 24, 34. The complete instrument is shown in fig. 2.

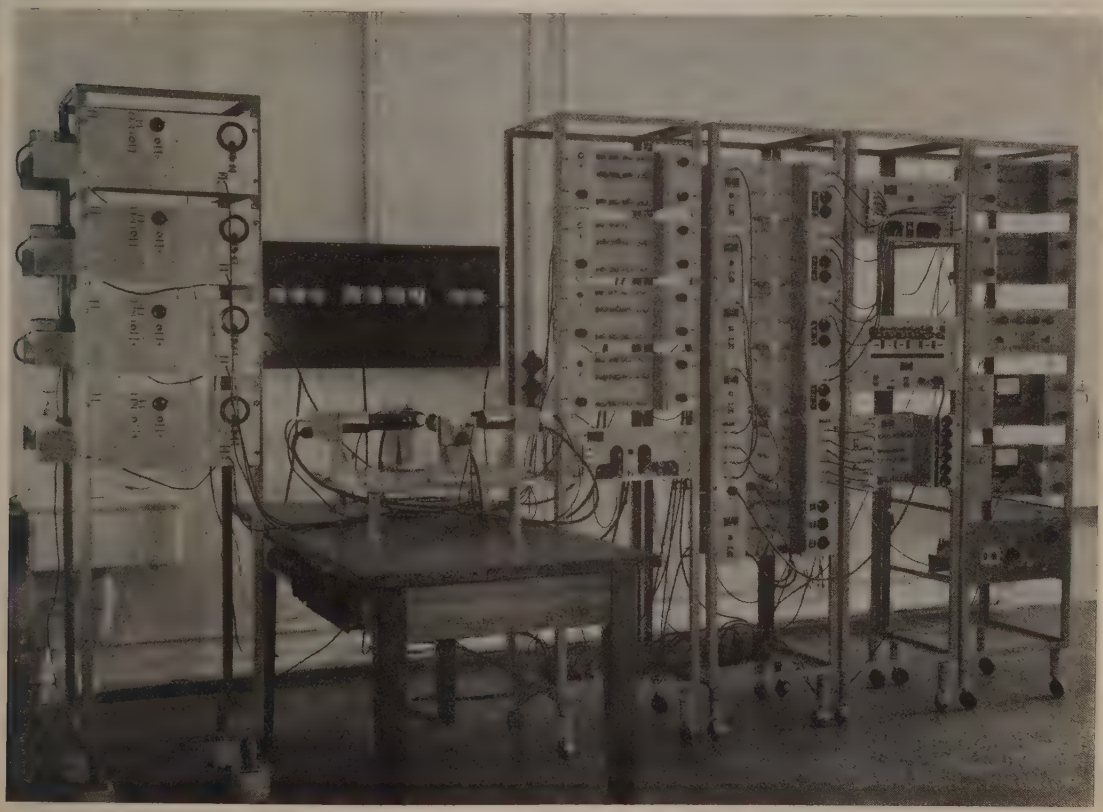

Fig. 2

In designing the electronic circuitry coincidence and gating resolving times of different parts of the circuit were adapted to the counting rates occurring in those parts. The resolving

time of the fast coincidence circuit, which accept *all* pulses from all four counters must be made as small as compatible with the inherent delay spread of pulses produced by scintillation counters with NaI (Tl) crystals. This resolving time was therefore put at about 0.1 μsec., as mentioned above. The conditioned gates that follow the limiting amplifiers each accept a full single channel counting rate. They must be conditioned so as to transmit only pulses from the fast coincidence circuit that truely coincide with single counts. These conditioned gates require a resolving time of about 0.5 μsec. At the coincidence matrix the input counting rate is only of the order of fast coincidence counting rate. Therefore the resolving time may be of the order of micro-seconds. Since in subsequent parts of the circuit counting rates become progressively lower and also because only truely coincident pulses remain, circuit requirements are progressively easier to fulfill.

3. Treament of Data

3.1. SYMMETRIC DETECTOR ARRANGEMENT

Let C_{ij} be the number of coincidences between gamma quantum γ_1 in detector i and gamma quantum γ_2 in detector j ($j > i$; $i, j = 1, 2, 3, 4$). Due to the action of the "coincidence cross delay" (cf. above) coincidences between γ_1 in detector j and γ_2 in detector i will also be recorded and are marked C_{ji}*. The anisotropy

$$A = \{C\,(180°) - C\,(90°)\}/C\,(90°)$$

then becomes

$$A = \sqrt[8]{\frac{(C_{13}\cdot C_{31}{}^{*}\cdot C_{24}\cdot C_{42}{}^{*})^2}{C_{12}C_{21}{}^{*}C_{23}C_{32}{}^{*}C_{34}C_{43}{}^{*}C_{14}C_{41}{}^{*}}} - 1.$$

Since

$$C_{ij} \approx C_{ji}{}^{*}$$

the following formula holds

$$A = \sqrt[4]{\frac{C_{13}{}^2\cdot C_{24}{}^2}{C_{12}\cdot C_{23}\cdot C_{34}\cdot C_{14}}} - 1$$

where now C_{ij} stand for the sum of the "direct" and "crossed" coincidences, i.e. $C_{ij} + C_{ji}$*, and are the six coincidence combinations recorded in the registers.

Instrumental parameters like solid angles, efficiencies of the counters, shapes of the spectral distributions and actual positioning of the lines *all cancel* because of the symmetric detector arrangement. Therefore, in spite of its rather complex electronic construction the MCG is not critical in adjustment and insensitive to minor instabilities.

It should be observed, that the strength of the source does not matter. The MCG is selfmonitoring. Contrary to conventional two-channel measurements no correction for source decay has to be applied and the source can be replaced by a stronger source or even be *continuously produced* during the cource of the measurements.

3.2. ASYMMETRIC DETECTOR ARRANGEMENTS

With only four detectors it becomes necessary to use an asymmetric arrangement in order to measure the complete angular correlation function $f(\theta)$. In this case the exact method described in the previous section can not be used. However $f(\theta)$ can be determined from the following expression

$$\frac{C_{ij}}{N_{i,\gamma 1}\cdot N_{j,\gamma 2} + N_{i,\gamma 2}\cdot N_{j,\gamma 1}} = g(t) f(\theta_{ij}) \qquad (3)$$

where N_{i,γ_1} etc. are the corresponding single channel counting rates. These single counting rates can be measured by reducing the fast coincidence bias until single counts are passed and alternatively connecting only one of the four counters.

The factor $g(t)$ is a time-dependent factor which is equal for all six coincidence combinations. We are only interested in the function $f(\theta)$. The factor $g(t)$ can therefore be treated as a constant. Also in this case the MCG is self-monitoring.

Formula (3) is not quite correct. In the general case N_{i,γ_1} etc. will consist not only of the desired pulses produced by gamma quantum γ_1 in detector i (signal) but also by undesirable background pulses caused by other gamma quanta emitted during the decay (noise). In (3) we have assumed that the signal to noise is approximately the same for all four detectors in both channels. The error introduced in this

way can easily be experimentally determined. If the detectors are all symmetrically arranged one can compare the results obtained from the correct formula (2) with those calculated from formula (3).

3.3 CORRECTIONS

The data have to be corrected for accidental coincidences. These may easily be determined from the resolving time of the fast coincidence circuit and the single counting rates.

Finally corrections for the finite solid angles of the detectors should also be applied just as in ordinary angular correlation measurements.

4. Applications

The MCG is primarily meant for angular correlation measurements on very short lived isotopes. The instrument is very suitable for this purpose partly because of the self-monitoring effect, discussed above, and partly because the coincidence counting efficiency is considerably higher than in a conventional arrangement. The measurement can therefore be done much faster. Our present four counter arrangement improves the coincidence counting efficiency by a factor of 12, when the six different coincidence combinations correspond to six different angles. In a symmetrical arrangement the efficiency gain will be slightly lower because the same angle will appear several times in different combinations. In the most unfavourable case (all counters 90° apart) this angular degeneracy reduces the gain factor to 10.7.

As a preliminary experiment the well-known Co^{60} cascade, 1.17–1.33 MeV, was measured. The anisotropy was found to be $18 \pm 4\%$. For the Bi^{207} cascade, 1.06–0.57 MeV, we obtained an anisotropy of $35 \pm 5\%$. Both results are in accordance with published values.

The authors are indebted to Professor Kai Siegbahn for his great interest in this work.

NUCLEAR INSTRUMENTS 1 (1957) 112; NORTH-HOLLAND PUBLISHING CO. – AMSTERDAM

BOOK REVIEW

The Physics of Nuclear Reactors, Brit. J. Appl. Phys. Suppl. No. 5.

Sir John Cockcroft says in his foreword to this book, "The papers published in this supplement, with the discussion on them, comprise the proceedings of a Conference arranged by The Institute of Physics in collaboration with the British Nuclear Energy Conference and held in London from 3 to 6 July, 1956. The purpose of the Conference was to keep members of the Institute and its sister Institutions abreast of scientific developments in nuclear reactors and to call their attention to the problems needing solution. The Conference was paritcularly intended for industrial and government physicists, working or likely to work directly or indirectly with reactors, and for lecturers and other teachers. Close on five hundred persons attended the Conference, including many from oversea. I commend this supplement as a useful record of the present state of our knowledge and the gaps which need to be filled".

In his opening address, 'Scientific problems in the development of nuclear power', Sir John Cockcroft outlines the varying problems to be solved in physics, chemistry and metallurgy.

The next paper, 'The physics of advanced reactors', by Dr. J. R. Dietrich, Argonne National Laboratory, U.S.A., is pherhaps the most interesting one. It discusses different types of thermal and fast reactors in terms of the neutron-physics characteristics of their moderators, coolant, and fuel cycles and the effects of the design objectives on power cost.

'Experimental reactor physics' by Mr P. W. Mummery discusses various integral measurements such as can be carried out with sub-critical, and low-power and high-power critical reactor assemblies.

'The zero-energy fast breeder reactor, ZEPHYR' by Dr. L. R. Shepherd describes the design of the reactor and experiments which have been carried out on it.

At an evening session Prof. R. E. Peierls delivered a lecture on 'Recent developments in nuclear theory'. As this lecture was a little outside the scope of the conference, only the headlines are given.

These papers on general reactor physics are followed by a number of papers on special topics.

Dr. A. H. Cottrell: The effects of irradiation on the physical properties of solids. Dr. G. C. Laurence: Shielding for reactors. Dr. A. J. Salmon: the control of reactors. Mr W. Macrae: The instrumentation of reactors. Dr. R. Spence: The role of chemistry in a nuclear energy project. Mr L. Rotherham: The role of metallurgy in a nuclear energy project.

The last two papers are: Dr. W. B. Lewis: The Canadian research reactors and their uses. Mr F. W. Fenning: The United Kingdom research reactors and their uses.

Most of the papers are followed by discussions.

As the conference was not primarily intended to report original research, most of the theoretical and experimental material of the papers has been published earlier, especially in the Proceedings of the International Conference on the Peaceful Uses of Atomic Energy in Geneva 1955. However, some new information is also presented, particularly in the discussions, not only from the United Kingdom but also from other countries. As regards existing reactors and reactors being designed in the United Kingdom and Canada a good survey of the present position is given.

INGVAR CARLVIK

PLASTIC PHOSPHOR NE 102

WE HAVE PLEASURE IN ANNOUNCING A NEW SCINTILLATOR, THE MOST EFFICIENT AND THE LOWEST COST PLASTIC PHOSPHOR EVER OFFERED.
(60-65% OF ANTHRACENE)
STANDARD SIZE RODS UP TO 24″ DIAMETER NOW AVAILABLE FROM STOCK

For the accommodation of Universities and laboratories, we can also supply NE 102 in rough ingot form at considerably reduced cost. Write for full details given in BULLETIN 11

NEW PRODUCTS AND SERVICES
(described in Bulletins 6 and 9)

- Scintillating Gels, for efficient internal counting of suspended materials
- Boron, Cadmium, Gadolinium and Lead Loaded Liquid Scintillators for neutron detection, or for enhanced gamma response
- Liquid Phosphors — Encapsulated, or in bulk form at new low prices
- Nuclear equipment built to your specifications

NUCLEAR ENTERPRISES (G.B.) Limited

BANKHEAD MEDWAY — SIGHTHILL — EDINBURGH, 11 — SCOTLAND
Telephone: CRAiglockhart 4513 – Cables: NUCLEAR

Associate Company: Nuclear Enterprises Limited — 1750 Pembina Highway — Winnipeg (Canada)

RADIATION INSTRUMENT CO.
MODEL 412 MERCURY RELAY

Precision Sliding Pulser

for Precise Calibration of Single & Multi-Channel Pulse Height Analyzers

Determines Window Widths Using Principle of *Constant Angular Velocity* } **AUTOMATICALLY 10 × more accurately 40 × faster than conventional pulsers**

Incorporates Both Manual Control and Precision Motor Drive

Simulates Pulses from Scintillation, Proportional, or Geiger Counters

RISE TIME—Less than .003 microsec.

DECAY TIME CONSTANT—1, 10, 100, 350, microsec. (selector switch).

PULSE AMPLITUDE—Continuously variable from 0 to maximum. Ranges 2, 3, 10, 30, 100, 1000 mV. Provision for direct connection of external battery for larger pulses.

POLARITY—Polarity switch permits selection of positive or negative pulses.

CALIBRATION—Self contained standard cell and null indicating balance circuit for precision adjustment.

LINEARITY—0.1% 10 turn Helical potentiometer with 5″ dial.

SCAN SPEED—2 RPM standard (1, 3, 5, 6 and 10 rpm also available.)

PRICE $ 450.00 f.o.b. SILVER SPRING, Md., U.S.A.

RADIATION INSTRUMENT CO.
P. O. BOX 733 SILVER SPRING, MARYLAND, U.S.A.

Just out

RELAXATION SPECTROMETRY

by

E. G. RICHARDSON

Professor of Acoustics and Reader in Physics
Physics Department, King's College, in the University of Durham

vii + 140 pages 89 illus. Guilders 20.— (40 s)

The object of the book is to determine a spectrum of acoustical frequencies at which the internal losses or relaxations exhibit maxima. Apart from the application of steady displacements the phenomena concern all frequencies from infra- to ultrasonic.

CONTENTS

I. Introduction. – II. Relaxational Behaviour, *Illus. by Models* **– III. The Infrasonic Spectrum – IV. The Sonic Spectrum – V. Ultrasonic Spectrum VI. Ultrasonic Range – VII. Dielectric Relaxation – VIII. Spectrum Analysis**

NORTH HOLLAND PUBLISHING COMPANY
AMSTERDAM

Cary / instrument abstracts

Applied Physics Corporation/Pasadena/California

Radioactivity Measurements Made Faster, Cheaper with Vibrating Reed Electrometer

Measurement of radioactivity in radioisotope determination, reactor control, air contamination studies, oil well logging, and other problems involving precise measurement of small currents, voltages and charges, such as precise pH determination and mass spectrometry, can now be made faster, simpler and cheaper by using the Cary Model 31 Vibrating Reed Electrometer.

Unusually high sensitivity plus high zero stability and ease of installation and operation are responsible for the greater speed and savings. The Model 31 detects as little as 10^{-17} amperes, and measures up to 10^{-6} amperes with a precision of 1%. Zero drift is less than 0.2 mV in 24 hours and less than .02 mV per hour.

C^{14}, H^3 DETERMINATIONS SIMPLIFIED

One widespread application in which the Model 31 has been of particular value is in determining C^{14}, H^3, and S^{35}. Wilzbach and his coworkers at Argonne National Laboratory have developed procedures* which simplify these determinations in a wide variety of organic compounds. Samples are converted directly to a gas suitable for measurement with an ionization chamber and the Model 31. This simple procedure eliminates the necessity for use of a precipitate, with its inaccuracy and time-consuming, tedious preparation.

Since as little as 10^{-12} curies of radioactivity can be detected, use of expensive "tagged" materials can be greatly reduced, often enough to return the cost of the instrument in a relatively short time.

The Model 31 can be used in any laboratory and does not require costly, vibration-free mountings or other special conditions of installation or operation. For additional information on the Model 31, write for bulletin NU-1 today. It gives you details on applications, references, performance, operating principle, specifications, modifications, accessories.

*Wilzbach, Brown, Kaplan, Science, **118**, 522-523 (1953)
Wilzbach, Van Dyken, Kaplan, Anal. Chem., **26**, 880 (1954)
Wilzbach, Sykes, Science **120**, 494-496 (1954).

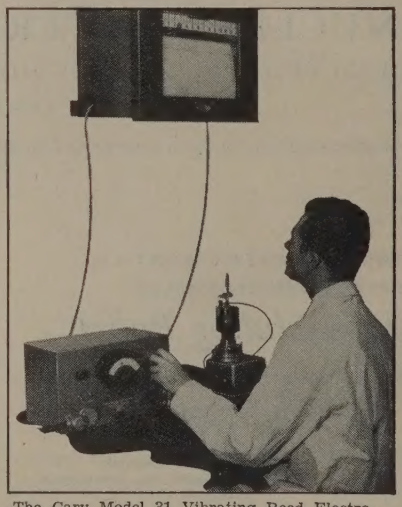

The Cary Model 31 Vibrating Reed Electrometer is capable of detecting a current as small as 1.0 X 10^{-17} amperes originating in a high impedance source. Charges as small as 5 X 10^{-16} coulombs and voltages as small as .02 mV can be measured.

CARY MODEL 36 VIBRATING REED AMPLIFIER IMPROVES MASS SPECTROMETER PERFORMANCE

The Cary Vibrating Reed Amplifier, Model 36, is being used in an increasing number of mass spectrometer installations where high molecular weight analyses make rapid scanning of mass numbers desirable. The Model 36 combines rapid response with high sensitivity. Response is critically damped, with an 0.1 sec. natural period (98.6 percent response in 0.1 second). Thus a range of 100 mass numbers can be accurately scanned in as little as one minute. Sensitivity and range are such that as little as 10^{-15} amperes and up to 10^{-11} amperes can be measured to a reproducibility of 0.2 percent without change of range. The stability of the Model 36 is superior too–zero drift is less than 10^{-15} amperes.

The Model 31 is preferred for mass spectrometer applications where extreme response speed is not required, such as isotope determinations. Sensitivity of the Model 31 is 10^{-17} amperes, and like the 36 it has high stability–less than 5 x 10^{-17} amperes zero drift.

Cary instruments:
SPECTROPHOTOMETERS · RAMAN SPECTROPHOTOMETER · ELECTROMETERS
VIBRATING REED AMPLIFIERS · INFRARED ANALYZERS · ULTRAVIOLET ANALYZERS

APPLIED PHYSICS CORPORATION / 362 WEST COLORADO STREET / PASADENA 1 / CALIFORNIA